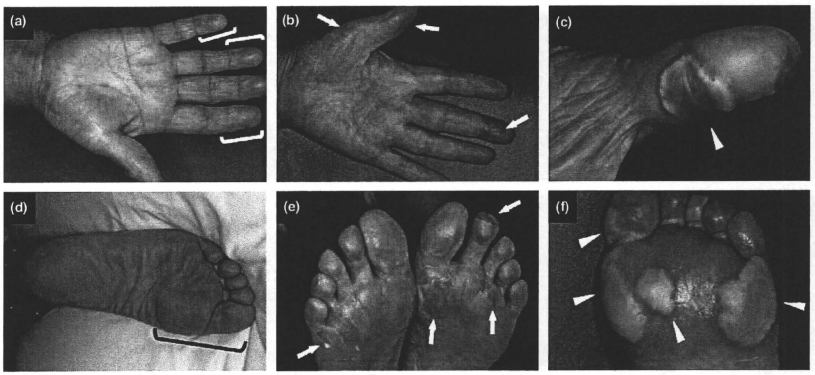

Figure 1. Photos of hand–foot syndrome (HFS) in Japanese patients treated with sorafenib. (a,d) Grade 1, (b,e) grade 2 and (c,f) grade 3. In grade 1 HFS, only mild erythema is found on the palmar and the plantar surface (brackets in a,d). In grade 2 HFS, peeling is observed at palmar and plantar pressure areas in addition to erythema (arrows in b,e). In grade 3 HFS, blisters with severe dermatitis around them are observed at palmar and plantar pressure area (arrowheads in c,f).

Table 2. Patient characteristics

	Study A (Akaza *et al.*, 2007)	Study B (Minami *et al.*, 2008)	Study C (Furuse *et al.*, 2008)
No. of patients	131[†]	31	27
Sex (*n*)			
Male	102	21	25
Female	29	10	2
Age (years)			
Median	63	63	70
Range	30–83	32–72	48–79
ECOG-PS (*n*)			
0	102	8	27
1	29	23	0
Cancer type (*n*)	Renal cell (131)	Non-small lung (10) Colorectal (6) Renal cell (3) Gastric (2) Others (10)	Hepatocellular (27)

[†]Number of patients considered valid for safety study was 131, while that for intent-to-treat was 129. ECOG-PS, Eastern Cooperative Oncology Group – performance status.

available for analyses. Patient characteristics of each of the three clinical trials are summarized in Table 2. No HFS was listed as a baseline characteristic in any of the patients. Underlying malignancies for the three studies included renal cell cancer, non-small cell lung cancer, hepatocellular cancer, and other cancers. Among patients receiving sorafenib, the summary incidence of all-grade HFS was 51% (55% in study A, 39% in B and 44% in C) and that of grade 3 HFS was 7% (9% in study A, 0% in B and 7% in C). HFS was one of the most frequently observed skin toxicities, along with rash/desquamation, in each of the three clinical trials (Table 3). In studies B and C, where sorafenib was administrated at different doses, dose

Table 3. Incidence of skin toxicities, including hand–foot syndrome (HFS)

	Study A (Akaza *et al.*, 2007)	Study B (Minami *et al.*, 2008)	Study C (Furuse *et al.*, 2008)	Total
	n = 131	*n* = 31	*n* = 27	*n* = 189
Adverse events	*n* (%)			
HFS				
Any grade	72 (55)	12 (39)	12 (44)	96 (51)
Grade 3	12 (9)	0	2 (7)	14 (7)
Alopecia				
Any grade	51 (39)	8 (26)	5 (19)	64 (34)
Grade 3/4	0	0	0	0
Dry skin				
Any grade	4 (3)	7 (23)	3 (11)	14 (7)
Grade 3/4	0	0	0	0
Pruritus				
Any grade	14 (11)	5 (16)	8 (30)	27 (14)
Grade 3/4	0	0	0	0
Rash/desquamation				
Any grade	49 (37)	19 (61)	15 (56)	83 (44)
Grade 3/4	5 (4)	0	2 (7)	7 (4)

Table 4. Incidence of hand–foot syndrome at different dose of sorafenib

	Study A (Akaza *et al.*, 2007)	Study B (Minami *et al.*, 2008)	Study C (Furuse *et al.*, 2008)
Dose	*n* = 131	*n* = 31	*n* = 27
100 mg b.i.d.	–	0/3 (0%)	–
200 mg b.i.d.	–	3/15 (20%)	4/13 (31%)
400 mg b.i.d.	72/131 (55%)	3/6 (50%)	8/14 (57%)
600 mg b.i.d.	–	6/7 (86%)	–

dependency for the incidence of HFS was suggested (Table 4). Incidence at 400 mg b.i.d. was similar among the three studies.

Timing of onset

An analysis of cumulative event rates of HFS in study A revealed that HFS occurred at the early stage of sorafenib treatment. Of the 72 patients suffering from sorafenib-related HFS, 43 patients developed new-onset HFS during the first 3 weeks of treatment, 14 patients at week 6, nine patients at week 9, and fewer thereafter (Fig. 2). A similar pattern was observed in the other clinical trials (data not shown).

HFS and patient characteristics

Incidence and severity of HFS in study A were summarized with respect to patient characteristics, including sex, age, Eastern Cooperative Oncology Group – performance status (ECOG-PS) and bodyweight (Table 5). None of the patient characteristics analyzed showed any apparent association with the incidence of all-grade HFS. Female sex (21% vs 6%) and ECOG-PS 0 (11% vs 3%) seemed to have a tendency to be related to grade 3 HFS; however, as there were great differences in patient numbers between women and men (29 vs 102) and between ECOG-PS 0 and 1 (102 vs 29), further investigations are needed to discern the relationship between these patient characteristics and severity of HFS.

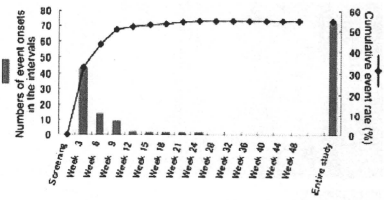

Figure 2. Timing of onset and cumulative event rate of hand–foot syndrome (HFS) in Japanese patients treated with sorafenib. HFS occurred at the early stage of sorafenib treatment. Out of 72 patients who had HFS in study A, 43 patients developed HFS during the first 3 weeks.

Table 5. Incidence of hand–foot syndrome by patient characteristics in study A

Patient characteristics	All grade *n* (%)	Grade 3 *n* (%)
Sex		
Male (*n* = 102)	51 (50)	6 (6)
Female (*n* = 29)	21 (72)	6 (21)
Age (years)		
<45 (*n* = 7)	3 (43)	0
45–64 (*n* = 68)	41 (60)	6 (9)
65–74 (*n* = 45)	20 (44)	4 (9)
≥75 (*n* = 11)	8 (73)	2 (18)
ECOG-PS		
0 (*n* = 102)	56 (55)	11 (11)
1 (*n* = 29)	16 (55)	1 (3)
Bodyweight (kg)		
<60 (*n* = 52)	30 (58)	5 (10)
60–69 (*n* = 52)	25 (48)	5 (10)
70–79 (*n* = 19)	13 (68)	2 (11)
≥80 (*n* = 7)	4 (57)	0

ECOG-PS, Eastern Cooperative Oncology Group – performance status.

Dose modification of sorafenib caused by HFS

In study A, HFS was the leading cause of dose interruption (14 patients, 11%) and dose reduction (12 patients, 9%) of sorafenib. HFS caused permanent discontinuation of sorafenib treatment in one patient (1%) in study A, but none in studies B and C.

DISCUSSION

The present analyses demonstrated that sorafenib was associated with a significantly increased risk of HFS in Japanese patients being treated for renal cell cancer and other solid tumors. The incidence of all-grade HFS (51%) was slightly higher than those reported overseas in phase III trials for RCC (30%) and HCC (21%), but the incidence of grade 3 HFS (7%) was comparable with those reported overseas in phase III trials (6% in RCC and 8% in HCC) or the systematically reviewed data of HFS incidence.[4,8,9] This suggests that there is no apparent racial difference in HFS incidence between white and Japanese subjects.

Hand–foot syndrome itself is not a new manifestation under treatment with chemotherapeutic agents. It has been reported that HFS is associated with several systemic chemotherapeutic agents including 5-fluorouracil, capecitabine, doxorubicin and others.[10–13] On the one hand, HFS observed in sorafenib treatment shares many features with conventional HFS (i.e. palm–plantar distribution, dose dependency, tenderness and impact on consistent antineoplastic therapy). On the other hand, it was reported that HFS associated with sorafenib differed from classical-type HFS in clinical and histological characteristics (sorafenib HFS is characterized by thick, well-defined hyperkeratotic lesions frequently affecting digit flexural locations).[14–16]

The pathogenesis of sorafenib-induced HFS is uncertain; however, for HFS observed in other systemic chemotherapeutic agents,[10] some hypotheses have been proposed: (i) excretion of cytotoxic drugs in sweat causes palms and soles to be more prone to HFS due to the higher number of eccrine sweat glands in the extremities, while areas with apocrine sweat glands are not affected;[11,12] (ii) a more mechanical effect of direct pressure to the areas affected, because sorafenib is a tyrosine kinase inhibitor affecting both VEGF and PDGF, the capillary endothelium may therefore be the first tissues damaged by sorafenib, especially the hand and foot surfaces which are under direct pressure from walking, hand washing or other daily use;[13] (iii) a direct effect of sorafenib on receptors located on the eccrine glands themselves; and (iv) alteration of keratinocytes by inhibition of the c-Kit receptor, because it has been shown that the c-Kit ligand is expressed on human keratinocytes,[17] and it is reasonable that the direct inhibiting effect of sorafenib on c-Kit may be toxic to the keratinocytes. In any case, dose-dependency of sorafenib-associated HFS does not suggest an allergic mechanism but a toxic one.[18] The significant incidence and risk demonstrated in this study underscore a need for additional basic and clinical studies to investigate the pathogenesis and treatment of sorafenib-associated HFS.

Although we investigated the relationships between patient characteristics and HFS, we found no such characteristic as related to HFS. Therefore, physicians need to pay attention to prevention and management of HFS in all sorafenib-treated patients. Recently, avoiding mechanical skin stimuli, moisturizing skin and manicure/pedicure of hyperkeratinized skin have been recommended to prevent occurrence and worsening of HFS.[15] In the present review, female and ECOG-PS 0 patients showed a higher tendency to be related to grade 3 HFS than male and ECOG-PS 1 patients, suggesting that the former patients may be more exposed to mechanical stimuli in daily life, such as washing dishes with hot water or active walking. As for topical treatment for prevention and management of HFS, moisturizing creams, urea- or salicylic acid-containing topical treatments for chemical exfoliation of skin, and topical corticosteroids for more severe inflammation with painful erythema, are recommended according to the skin symptoms.[15]

Once HFS is observed, dose modification of sorafenib is one of the options in management of HFS, along with physical and chemical therapies. Although the first step in dose modification of sorafenib was dose interruption in the three clinical trials, recently published articles recommend the treatment algorithm of HFS in which the first step in dose modification of sorafenib should be dose reduction instead of dose interruption.[16,19] In order to fulfill the antitumor effect of sorafenib, it is important to

maintain sorafenib exposure. For that purpose, it is reasonable to reduce sorafenib dose instead of interrupting sorafenib treatment as the first step of dose modification.

In conclusion, the present review has demonstrated that sorafenib was associated with a relatively high risk of developing HFS, and HFS was one of the most frequently observed skin toxicities along with rash/desquamation in Japanese patients. As none of the baseline patient characteristics was predictive of HFS, physicians should pay attention to prevention and management of HFS in all sorafenib-treated patients in order to avoid treatment interruption/discontinuation of sorafenib due to HFS.

ACKNOWLEDGMENT

The clinical trials reviewed here were supported by Bayer Yakuhin, Osaka, Japan.

REFERENCES

1 Wilhelm SM, Carter C, Tang L *et al.* BAY 43-9006 exhibits broad spectrum oral antitumor activity and targets the RAF/MEK/ERK pathway and receptor tyrosine kinases involved in tumor progression and angiogenesis. *Cancer Res* 2004; **64**: 7099–7109.

2 Carlomagno F, Anaganti S, Guida T *et al.* BAY 43-9006 inhibition of oncogenic RET mutants. *J Natl Cancer Inst* 2006; **98**: 326–334.

3 Akaza H, Tsukamoto T, Murai M, Nakajima K, Naito S. Phase II study to investigate the efficacy, safety, and pharmacokinetics of sorafenib in Japanese patients with advanced renal cell carcinoma. *Jpn J Clin Oncol* 2007; **37**: 755–762.

4 Chu D, Lacouture ME, Fillos T, Wu S. Risk of hand-foot skin reaction with sorafenib: a systematic review and meta-analysis. *Acta Oncol* 2008; **47**: 176–186.

5 Minami H, Kawada K, Ebi H *et al.* Phase I and pharmacokinetic study of sorafenib, an oral multikinase inhibitor, in Japanese patients with advanced refractory solid tumors. *Cancer Sci* 2008; **99**: 1492–1498.

6 Furuse J, Ishii H, Nakachi K, Suzuki E, Shimizu S, Nakajima K. Phase I study of sorafenib in Japanese patients with hepatocellular carcinoma. *Cancer Sci* 2008; **99**: 159–165.

7 National Cancer Institute (NCI). *Common Toxicity Criteria v2.0 and Common Terminology Criteria for Adverse Events v3.0.* [Accessed 2 July 2009.] Available from http://ctep.cancer.gov/reporting/ctc.html

8 Escudier B, Eisen T, Stadler WM *et al.* Sorafenib in advanced clear-cell renal-cell carcinoma. *N Engl J Med* 2007; **356**: 125–134.

9 Llovet JM, Ricci S, Mazzaferro V *et al.* Sorafenib in advanced hepatocellular carcinoma. *N Engl J Med* 2008; **359**: 378–390.

10 Meta-Analysis Group in Cancer. Toxicity of fluorouracil in patients with advanced colorectal cancer: Effect of administration schedule and prognostic factors. *J Clin Oncol* 1998; **16**: 3537–3541.

11 Mrozek-Orlowski ME, Frye DK, Sanborn HM. Capecitabine: nursing implications of a new oral chemotherapeutic agent. *Oncol Nurs Forum* 1999; **26**: 753–762.

12 Jacobi U, Waibler E, Schulze P *et al.* Release of doxorubicin in sweat: first step to induce the palmar-plantar erythrodysesthesia syndrome? *Ann Oncol* 2005; **16**: 1210–1211.

13 Lorusso D, Di Stefano A, Carone V, Fagotti A, Pisconti S, Scambia G. Pegylated liposomal doxorubicin-related palmar-plantar erythrodysesthesia ('hand-foot' syndrome). *Ann Oncol* 2007; **18**: 1159–1164.

14 Robert C, Soria JC, Spatz A *et al.* Cutaneous side-effects of kinase inhibitors and blocking antibodies. *Lancet Oncol* 2005; **6**: 491–500.

15 Robert C, Mateus C, Spatz A, Wechsler J, Escudier B. Dermatologic symptoms associated with the multikinase inhibitor sorafenib. *J Am Acad Dermatol* 2009; **60**: 299–305.

16 Autier J, Escudier B, Wechsler J, Spatz A, Robert C. Prospective study of the cutaneous adverse effects of sorafenib, a novel multikinase inhibitor. *Arch Dermatol* 2008; **144**: 886–892.

17 Morita E, Lee DG, Sugiyama M, Yamamoto S. Expression of c-kit ligand in human keratinocytes. *Arch Dermatol Res* 1994; **286**: 273–277.

18 Azad NS, Aragon-Ching JB, Dahut WL *et al.* Hand-foot skin reaction increases with cumulative sorafenib dose and with combination anti-vascular endothelial growth factor therapy. *Clin Cancer Res* 2009; **15**: 1411–1416.

19 Lacouture ME, Wu S, Robert C *et al.* Evolving strategies for the management of hand-foot skin reaction associated with the multitargeted kinase inhibitors sorafenib and sunitinib. *Oncologist* 2008; **13**: 1001–1011.

Cancer Science
The official journal of the Japanese Cancer Association JCA

Phase I dose escalation and pharmacokinetic study of oral enzastaurin (LY317615) in advanced solid tumors

Toru Mukohara,[1,4] Shunji Nagai,[1] Minori Koshiji,[2] Kenichi Yoshizawa[2] and Hironobu Minami[1,3,4]

[1]Division of Oncology/Hematology, National Cancer Center Hospital East, Kashiwa; [2]Eli Lilly Japan KK, Kobe, Japan

(Received March 9, 2010/Revised June 24, 2010/Accepted June 25, 2010/Accepted manuscript online July 13, 2010/Article first published online August 17, 2010)

Enzastaurin is an oral serine/threonine kinase inhibitor that targets the protein kinase C (PKC) and phosphoinositide 3-kinase/AKT pathways to induce apoptosis and suppress proliferation of various cancer cell lines. This phase I study evaluated the tolerability and pharmacokinetics of enzastaurin in Japanese patients with advanced solid tumors and determined the recommended dose for phase II. Eligible patients had advanced solid tumors and an Eastern Cooperative Oncology Group performance status of 0–2. Patients received enzastaurin orally once daily until disease progression (PD) or unacceptable toxicity occurred. Enzastaurin was started at 250 mg/day followed by stepwise dose increases based on the incidence of dose-limiting toxicities (DLT). Twenty-three patients (seven patients: 250 mg; six patients: 375 mg; six patients: 500 mg; four patients: 750 mg) were enrolled and received enzastaurin. The major tumor types were non-small-cell lung cancer (n = 5) and breast cancer (n = 3). No DLT was reported at doses of 500 mg or less. Because two DLT (grade 2 QTc prolongation lasting for a week) were observed at 750 mg enzastaurin, this was determined as the maximum tolerated dose. Multiple daily doses at 500 mg achieved the target plasma concentration to inhibit PKC activity (1400 nmol/L). Enzastaurin was well tolerated up to 500 mg in Japanese patients with advanced solid tumors. The recommended dose for phase II was determined to be 500 mg daily for a 28-day cycle on the basis of safety and plasma exposures. (*Cancer Sci* 2010; 101: 2193–2199)

Protein kinase C (PKC) is overexpressed and its activity is increased in many cancers including colon cancer,[1] non-small-cell lung cancer (NSCLC)[2] and diffuse large B-cell lymphoma (DLBCL).[3] Protein kinase C is stimulated on activation of receptors on the cell membrane, including vascular endothelial growth factor (VEGF) and epidermal growth factor (EGF).[4] Recent evidence suggests a link between PKC and phosphoinositide 3-kinase (PI3K)/AKT, the main pathway responsible for cell survival and proliferation.[5,6]

Enzastaurin is an oral serine/threonine kinase inhibitor that targets the PKC and PI3K/AKT pathways to induce apoptosis and suppress proliferation of various cancer cell lines.[1,7,8] In animal models, enzastaurin showed antitumor and antiangiogenic activity in various malignancies, including NSCLC, colon cancer, renal cell cancer, hepatocellular cancer and glioblastoma.[1,9,10] Enzastaurin has been well tolerated in an early clinical study conducted in the USA at doses from 20 to 750 mg/day in patients with advanced solid tumors.[11]

Enzastaurin is primarily metabolized by cytochrome P450 3A (CYP3A), leading to the formation of multiple metabolites, including three active metabolites: a desmethylenepyrimidyl metabolite (LY326020); a desmethyl metabolite (LY485912); and a hydroxymethyl intermediate (LSN2406799). These metabolites are pharmacologically active, inhibiting PKC-β with similar potencies to enzastaurin (IC_{50} approximately 6 nmol/L) (data on file).[12] Results from *in vitro* studies have shown that enzastaurin inhibits 90% of PKC-β enzymatic activity (IC_{90}) at 70 nmol/L (data on file). Since preliminary data suggest that plasma protein binding of enzastaurin is approximately 95%, total plasma concentrations above 1400 nmol/L would be required to achieve 70 nmol/L or higher of the free concentration.

Here we report the results of a phase I study that was conducted to evaluate the tolerability of enzastaurin and its pharmacokinetic profile in Japanese patients with advanced solid tumors. Based on these results we have also determined the recommended dose of enzastaurin for a planned phase II study, and evaluated the antitumor effect of enzastaurin in these patients.

Patients and Methods

Patients. Patients with histologically or cytologically confirmed malignant solid tumor, refractory to conventional chemotherapy or available non-standard therapy and without any carry-over influence of previous therapies, were eligible to enter the study. Inclusion criteria included the following: age between 20 and 75 years; Eastern Cooperative Oncology Group (ECOG) performance status (PS) from 0 to 2; predicted life expectancy of at least 3 months; and adequate hematopoietic, hepatic and renal functions (absolute neutrophil counts $\geq 1.5 \times 10^3/mm^3$, platelets $\geq 100 \times 10^3/mm^3$, hemoglobin ≥ 9 g/dL, total bilirubin $\leq 1.5 \times$ upper limit of normal [ULN], aspartate aminotransferase [AST] and alanine amino-transferase [ALT] $\leq 2.5 \times$ ULN, and serum creatinine $\leq 1.5 \times$ ULN). Exclusion criteria included the following: present cardiac disorders of grade 3 or greater; myocardial infarction within 6 months after onset; pleural, peritoneal or pericardial effusion requiring drainage; QTc ≥ 0.45 s (QTc = $QT/\sqrt{(R\text{-}R)}$ (Bazette); dissemination to the meninges; or history of stomach resection. Toxicity was graded in accordance with the National Cancer Institute Common Terminology for Adverse Events (CTCAE) ver. 3.0.

Ethical considerations. The study was conducted in accordance with the ethical principles of the Declaration of Helsinki and was consistent with Good Clinical Practice and all applicable laws and regulations. Written informed consent was obtained from all patients and the study was approved by the Institutional Review Board of the participating institution.

Study design. This was an open-label phase I dose-escalation study in one clinical center, the National Cancer Center Hospital East, Japan.

Five fixed dose levels of enzastaurin, 250, 375, 500, 750 and 1000 mg/day, were to be examined in the study. The starting dose, 250 mg enzastaurin, was selected based on the results from the previous phase I study of enzastaurin conducted in patients with advanced solid tumors.[11] In that study, 500 mg enzastaurin was the lowest daily dose at which dose-limiting toxicity (DLT) was observed. We therefore selected half that dose as the starting dose in this study. A six patient cohort was

[3]To whom correspondence should be addressed.
E-mail: hminami@med.kobe-u.ac.jp
[4]Present address: Medical Oncology/Hematology, Kobe University Graduate School of Medicine, Kobe, Japan.

doi: 10.1111/j.1349-7006.2010.01677.x

used for each dose level being escalated in a stepwise manner based on DLT incidence. The DLT was defined as any of the following occurring in cycle 1: grade 3, or higher non-hematological toxicity except nausea, vomiting, anorexia, fatigue, constipation, diarrhea and allergic reactions; grade 4 neutropenia or thrombocytopenia; febrile neutropenia; grade 2 QTc prolongation lasting at least 1 week; or dose omission lasting at least 8 days. Because preclinical study showed that enzastaurin could cause QTc prolongation in dogs and it was actually observed in the preceding phase I study in the USA, we defined sustained QTc prolongation as DLT even when it was grade 2, from a safety perspective. Nausea, vomiting, anorexia, fatigue, constipation and diarrhea were considered as DLT only when they persisted in grade 3 or higher despite adequate symptomatic treatment and the investigator judged them as DLT. The maximum tolerated dose (MTD) was defined as the lowest dose level where the incidence of DLT was 33% or higher. If there was a patient whose compliance was <75% and who experienced no DLT in cycle 1 at a certain dose level, an additional patient was enrolled at that dose level. A patient whose dose omission was <25% or who experienced DLT in cycle 1 was evaluable for DLT analysis. The incidence of DLT at each dose level was summarized using the patients evaluable for DLT.

Treatment plan. Enzastaurin was administered orally once daily after breakfast, because exposures of enzastaurin following administration in the fed state were higher than exposures following administration in the fasted state (data on file).

The study treatment consisted of two periods: cycle 0 and all subsequent cycles. In cycle 0, patients received a single dose of enzastaurin to investigate its pharmacokinetic profile. Cycle 1 was initiated during the period from 8 to 15 days following single-dose administration in cycle 0. During cycle 1 and the subsequent cycles (1 cycle = 28 days), patients received enzastaurin tablets once daily until disease progression (PD) or unacceptable toxicity occurred.

If any adverse event meeting DLT criteria occurred, the patient was required to omit the administration of enzastaurin until the event resolved or improved to grade 1. If the patient restarted the study treatment, the dose of enzastaurin was reduced to the next lowest level. For each patient, a maximum of two dose reductions were allowed.

Prohibited medications during the study period included Vaughan-Williams Class Ia, Ic and III antiarrhythmic drugs, CYP3A4 inhibitors, CYP3A4 inducers and warfarin.

Toxicity and response monitoring. The following measures were used to assess patients at pre-study and during treatment: body weight, PS, laboratory tests, vital signs, electrocardiogram (ECG), chest X-ray and ophthalmological examination results. Post-study evaluation was conducted 28 days after the last dose.

Adverse events were graded in accordance with CTCAE ver. 3.0. The antitumor effect was assessed using the Response Evaluation Criteria in Solid Tumors (RECIST)[13] for every other cycle, and was confirmed at least 4 weeks after the initial observation of responses.

Pharmacokinetics. During cycle 0, heparinized blood samples (3 mL) were collected 0.5, 1, 1.5, 2, 3, 4, 6, 9, 24, 48, 72, 96 and 168 h after the dose. During cycle 1, blood samples (3 mL) were collected pre-dose and 6 h post-dose on day 1; pre-dose on days 8, 15 and 22; and pre-dose, 0.5, 1, 1.5, 2, 3, 4, 6, 9 and 24 h post-dose on day 28.

High-performance liquid chromatography with tandem mass-spectrometry (LC/MS/MS) was used to detect enzastaurin and its metabolites, LY326020, LY485912 and LSN2406799, in plasma (Advion BioSciences, Ithaca, NY, USA).

The PK parameters for enzastaurin and its metabolites were analyzed using noncompartmental methods with WinNonlin Version 5.0.1. (Pharsight, Mountain View, CA, USA). The primary parameters, such as maximal concentration (C_{max}), time of maximal concentration (t_{max}), area under the plasma concentration *vs* time curve from 0 to 24 h ($AUC_{0-24\ h}$) and to infinity ($AUC_{0-\infty}$), apparent clearance (CL/F), apparent volume of distribution (Vz/F) and the apparent terminal half-life ($t_{1/2}$) were calculated during cycle 0. Similarly, during cycle 1, the maximum concentration at steady-state during a dosing interval ($C_{max,ss}$) and the time taken to reach $C_{max,ss}$ ($t_{max,ss}$) were identified. The area under the plasma concentration *vs* the time curve over the dosing interval at steady-state ($AUC_{\tau,ss}$) was determined. The linear/log trapezoidal method was used to compute AUC values. Other non-compartmental parameters such as predicted average drug concentration under steady-state conditions during a dosing interval ($C_{av,ss}$), apparent clearance (CL_{ss}/F) and apparent volume of distribution at steady-state (V_{ss}/F) were also calculated. The accumulation ratio (RA) was assessed as $AUC_{\tau,ss}$ to AUC_{0-24}. The metabolic ratio (MR) was calculated as metabolite AUC to parent AUC.

C_{max} and t_{max} values of total analytes (enzastaurin + LY326020 + LY485912 + LSN2406799) were reported by summing the concentration–time data for enzastaurin together with its metabolites, because these metabolites inhibit PKC-β with potencies similar to enzastaurin. If two or more of the individual values were not present, the value to be computed was indicated as missing.

The analysis to estimate intra-subject and inter-subject variability used data from cycle 0 and cycle 1. $AUC_{0-\infty}$ from single dosing was combined with $AUC_{\tau,ss}$ after multiple dosing. This combination strategy was based on linear pharmacokinetic principles that have shown "$AUC_{\tau,ss} \approx AUC_{0-\infty}$".

Results

Patient characteristics. This study was conducted from November 2005 to January 2008 at the National Cancer Center Hospital East in Japan and 23 patients were enrolled (Table 1).

Table 1. Patient characteristics (*N* = 23)

Patient characteristics	*N* = 23
Gender	
Male	15
Female	8
Age (years)	
Median	55.0
Range	27–71
ECOG performance status	
0	10
1	13
Diagnosis	
Non-small-cell lung cancer	5
Breast cancer	3
GIST	2
Renal cancer	2
Brain tumor	1
Gastric cancer	1
Intrahepatic bile duct cancer	1
Liposarcoma	1
Large intestine carcinoma	1
Malignant neoplasm of urachus	1
Malignant neoplasm of retromolar area	1
Pleural mesothelioma	1
Rectal cancer	1
Thyroid tumor and leiomyosarcoma	1
Carcinoma of unknown primary	1

ECOG, Eastern Cooperative Oncology Group; GIST, gastro-intestinal stromal tumor.

doi: 10.1111/j.1349-7006.2010.01677.x

Table 2. Toxicity possibly related to enzastaurin observed in >10% of patients

Preferred term (MedDRA ver.10.0)	Dose of enzastaurin (mg)									Total (N = 23)		
	250 (N = 7)		375 (N = 6)		500 (N = 6)		750 (N = 4)					
	G1	G2	G1	G2	G1	G2	G1	G2	G3	G1	G2	G3
Chromaturia	4	0	4	0	4	0	3	0	0	15	0	0
Somnolence	0	0	2	0	4	0	3	0	0	9	0	0
Faeces discoloured	2	0	2	0	0	0	1	0	0	5	0	0
Fatigue	0	1	1	0	1	0	0	1	0	2	2	0
ECG QTc interval prolonged	0	0	0	1	0	1	0	2	0	0	4	0
Blood albumin decreased	0	0	1	0	1	0	0	1	0	2	1	0
Blood urine present	0	0	1	1	1	0	0	0	0	2	1	0
Lymphocyte count decreased	0	0	0	2	0	0	0	0	1	0	2	1
Rash	0	1	0	1	0	1	0	0	0	0	3	0

ECG, electrocardiogram; G, grade of CTCAE v3.0; MedDRA, the Medical Dictionary for Regulatory Activities.

The most common types of cancer were NSCLC (n = 5) and breast cancer (n = 3).

Maximum tolerated dose and toxicity. All 23 patients received at least one enzastaurin dose. The median number of treatment cycles was two cycles at 250 mg, four at 375 mg, 2.5 at 500 mg and 2.5 at 750 mg. Twenty-one patients discontinued the study due to progressive disease and two patients discontinued due to adverse events. One patient at 250 mg experienced progressive disease before the end of the first cycle, so that patient was added to the cohort. One patient at 375 mg discontinued the study due to drug-related QTc prolongation and the other patient at 750 mg discontinued because of anorexia, which was not drug related.

Of 23 treated patients, four patients were excluded from DLT analysis because of early progression of their disease. The incidence of DLT was summarized by the enzastaurin dose in 19 patients (five patients at 250 mg, six patients at 375 mg, five patients at 500 mg and three patients at 750 mg). No DLT was reported at doses of 500 mg or less. Two DLT were reported at 750 mg; both were grade 2 QTc prolongations lasting at least 1 week. Based on the results, 750 mg of enzastaurin was determined as the MTD and 500 mg as the recommended dose for phase II studies.

Table 2 shows toxicities possibly related to enzastaurin that were observed in more than 10% of patients. The most common toxicities in the treated patients were chromaturia (n = 15) and somnolence (n = 9), which were both grade 1. The incidence of somnolence appeared to increase dose-dependently. The only grade 3 toxicity was lymphocytopenia (n = 1). There were no drug-related deaths.

Three patients (one at 375 mg and two at 750 mg) required dose omission due to grade 2 QTc prolongation, which was deemed as DLT in two of them. One patient at 375 mg experienced grade 2 QTc prolongation lasting for 8 days in cycle 2. All QTc prolongation events were reversible in these patients and they recovered from these events after dose omission. However, QTc prolongation events continued to occur again until sufficient dose reduction was taken (Fig. 1). The patient at 375 mg discontinued due to drug-related prolonged QTc interval, which occurred again even after a dose reduction to 250 mg (Fig. 1). The plasma concentration of enzastaurin and its active metabolites at the point of patients' experiencing QTc prolongation is not available.

Pharmacokinetics. Plasma concentration–time data and dosing information (dose date and time) for pharmacokinetic evaluation were available from 23 patients. Two patients at 750 mg were excluded from the analysis for steady-state because their enzastaurin doses were reduced during cycle 1 due to adverse events.

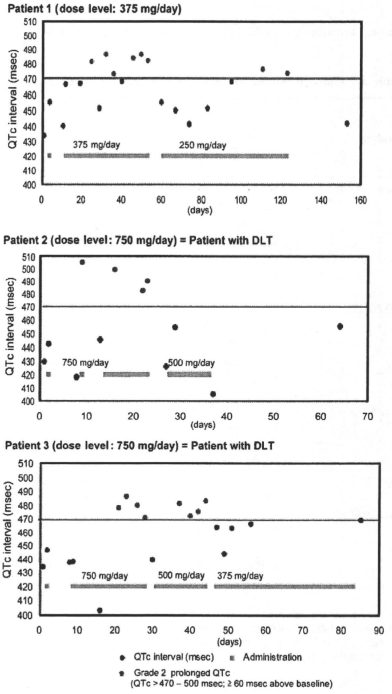

Fig. 1. Patients who required dose omission because of QTc prolongation. DLT, dose-limiting toxicities.

Figure 2 shows the mean plasma concentration–time profile of enzastaurin. The mean pharmacokinetic parameters of enzastaurin and its active metabolites following single and multiple

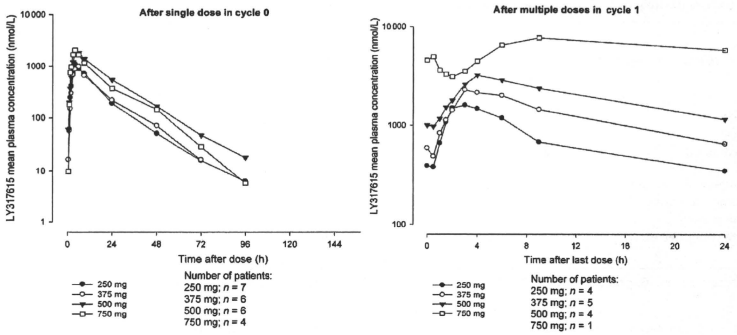

Fig. 2. Enzastaurin (LY317615) mean plasma concentration–time profile.

Table 3. Pharmacokinetic parameters of enzastaurin and its active metabolites in cycle 0

Analyte	Parameters	Geometric mean (coefficient of variation %)			
		Dose of enzastaurin (mg)			
		250	375	500	750
Enzastaurin	N	7	6	6	4
	C_{max} (nmol/L)	1090 (57.5)	968 (61.3)	2070 (40.2)	1910 (73.3)
	t_{max} (h)*	4.07 (2.87–8.92)	3.96 (3.00–6.10)	5.96 (3.00–9.03)	3.92 (3.15–4.00)
	$AUC_{0-\infty}$ (h μmol/L)	12.7 (78.7)	12.9 (77.6)	29.5 (70.2)	23.5 (96.6)
	CL/F (L/h)	38.0 (78.7)	56.4 (77.6)	32.9 (70.2)	61.9 (96.6)
	V_z/F (L)	651 (70.7)	820 (69.1)	632 (39.1)	957 (68.5)
	$t_{1/2}$ (h)†	11.9 (7.6–17.0)	10.1 (7.5–16.4)	13.3 (8.4–20.3)	10.7 (8.2–14.1)
LY326020	N	7	6	6	4
	C_{max} (nmol/L)	285 (36.7)	308 (24.3)	494 (39.9)	548 (53.1)
	t_{max} (h)*	5.77 (2.87–8.97)	5.01 (4.00–9.02)	9.02 (4.00–24.02)	5.00 (3.92–6.00)
	$AUC_{0-\infty}$ (h μmol/L)	12.2 (50.2)	14.6 (46.8)	27.8 (61.1)	26.3 (65.5)
	$t_{1/2}$ (h)†	38.2 (27.2–55.6)	34.8 (28.9–40.5)	37.8 (26.6–55.6)	38.4 (33.2–41.1)
	MR	0.961 (60.7)	1.13 (37.3)	0.942 (46.9)	1.12 (23.7)
LY485912	N	7	6	6	4
	C_{max} (nmol/L)	122 (57.3)	107 (48.8)	258 (50.2)	218 (77.7)
	t_{max} (h)*	5.77 (3.93–8.97)	6.10 (4.02–9.02)	9.02 (6.20–24.02)	5.00 (3.92–9.07)
	$AUC_{0-\infty}$ (h μmol/L)	2.25 (88.4)	2.17 (91.3)	5.88 (103)	4.54 (132)
	$t_{1/2}$ (h)†	12.0 (7.7–19.7)	10.5 (9.4–14.0)	12.6 (8.7–19.6)	11.5 (6.8–17.7)
	MR	0.176 (15.3)	0.168 (15.8)	0.199 (33.3)	0.193 (19.8)
LSN2406799	N	7	6	6	4
	C_{max} (nmol/L)	145 (34.0)	143 (41.3)	276 (31.8)	242 (92.8)
	t_{max} (h)*	4.02 (2.87–6.07)	3.96 (3.00–6.10)	4.96 (3.00–9.03)	3.92 (3.15–4.00)
	$AUC_{0-\infty}$ (h μmol/L)	1.40 (68.4)	1.49 (60.8)	3.25 (49.6)	2.71 (92.6)
	$t_{1/2}$ (h)†	10.5 (7.1–13.7)	8.70 (7.1–11.9)	11.6 (6.1–17.1)	10.3 (5.7–19.7)
	MR	0.110 (9.2)	0.115 (15.3)	0.110 (18.7)	0.115 (12.5)

*Median (range). †Geometric mean (range). $AUC_{0-\infty}$ area under the concentration *vs* time curve from 0 to infinity; CL/F, apparent total body clearance calculated after oral dosing; C_{max}, maximum plasma concentration; MR, metabolic ratio; t_{max}, median time to reach maximum concentration; $t_{1/2}$, half-life associated with the terminal rate constant; V_z/F, apparent volume of distribution after oral administration.

dosing are summarized in Tables 3 and 4, respectively. Mean concentration–time profile of enzastaurin after a single dose monophasically declined following C_{max} and the mean $t_{1/2}$ of enzastaurin ranged from 10.1 to 13.3 h independent of the dose administered. C_{max} and $AUC_{0-\infty}$ of enzastaurin did not increase dose-proportionally after a single dose or during multiple dosing. The RA of enzastaurin ranged from 1.19 to 3.56 and did not appear to be dose dependent.

LY326020 has a longer half-life than enzastaurin, indicating that this metabolite is elimination-rate limited. The RA of LY326020 ranged from 2.18 to 3.87, which tended to be higher due to its longer half-life. The MR of LY326020 ranged from 0.942 to 1.13 after single dosing and from 0.359 to 0.679 after multiple dosing. These results suggest that systemic exposure of LY326020 was similar to or slightly lower than that of enzastaurin. The mean $t_{1/2}$ of LY485912 and LSN2406799 were similar

doi: 10.1111/j.1349-7006.2010.01677.x

Table 4. Pharmacokinetic parameters of enzastaurin and its active metabolites in cycle 1

Analyte	Parameters	Geometric mean (coefficient of variation %)			
		Dose of enzastaurin (mg)			
		250	375	500	750
Enzastaurin	N	4	5	4	1
	$C_{max,ss}$ (nmol/L)	1460 (62.9)	1920 (83.1)	3230 (36.2)	7680†
	t_{max} (h)*	2.48 (1.92–3.95)	3.08 (3.00–6.08)	4.00 (3.00–6.07)	9.08†
	$AUC_{\tau,ss}$ (h μmol/L)	15.00 (98.1)	22.20 (122)	40.90 (61.6)	147.00†
	$C_{av,ss}$ (nmol/L)	624 (98.1)	927 (122)	1710 (61.6)	6140†
	CL/F (L/h)	32.4 (98.1)	32.7 (122)	23.7 (61.6)	9.87†
	RA	1.19 (88.4)	2.24 (45.0)	1.96 (48.4)	3.56†
LY326020	N	4	5	4	1
	$C_{max,ss}$ (nmol/L)	470 (38.3)	754 (48.0)	1260 (45.8)	2640†
	t_{max} (h)*	3.93 (1.42–4.00)	6.00 (3.08–9.13)	5.00 (0.52–24.00)	0.50†
	$AUC_{\tau,ss}$ (h μmol/L)	9.33 (39.4)	15.1 (55.9)	27.1 (52.9)	53.00†
	$C_{av,ss}$ (nmol/L)	389 (39.4)	629 (55.9)	1130 (52.9)	2210†
	MR	0.623 (60.0)	0.679 (54.6)	0.663 (23.4)	0.359†
	RA	2.18 (52.8)	2.90 (26.8)	3.87 (51.6)	3.78†
LY485912	N	4	5	4	1
	$C_{max,ss}$ (nmol/L)	188 (90.7)	253 (108)	490 (52.5)	1480†
	t_{max} (h)*	4.97 (3.92–9.93)	6.00 (4.03–9.00)	7.52 (6.00–24.00)	0.00†
	$AUC_{\tau,ss}$ (h μmol/L)	2.92 (125)	4.29 (148)	8.99 (67.5)	29.60†
	$C_{av,ss}$ (nmol/L)	121 (125)	179 (148)	374 (67.5)	1230†
	MR	0.195 (20.6)	0.193 (15.8)	0.220 (9.8)	0.201†
	RA	1.38 (119)	2.96 (48.5)	2.60 (38.5)	3.60†
LSN2406799	N	4	5	4	1
	$C_{max,ss}$ (nmol/L)	166 (53.2)	197 (51.2)	331 (17.6)	574†
	t_{max} (h)*	3.46 (1.92–3.95)	3.97 (3.00–9.13)	4.00 (3.00–6.07)	9.08†
	$AUC_{\tau,ss}$ (h μmol/L)	1.60 (75.9)	2.22 (85.3)	3.81 (43.1)	10.50†
	$C_{av,ss}$ (nmol/L)	66.6 (75.9)	92.4 (85.3)	159 (43.1)	436†
	MR	0.107 (21.3)	0.0997 (28.8)	0.0931 (17.2)	0.0710†
	RA	1.09 (63.1)	1.78 (40.7)	1.62 (38.2)	2.44†

*Median (range). †Individual values, mean and CV% were not calculated because $N \leq 2$. $AUC_{\tau,ss}$, area under the concentration *vs* time curve over the dosing interval at steady state; $C_{av,ss}$, the predicted average drug concentration under steady-state conditions during multiple dosing; $C_{max,ss}$, maximum plasma concentration at steady-state; MR, metabolic ratio; RA, accumulation ratio; t_{max}, median time to reach maximum concentration.

to that of enzastaurin. This indicates that elimination may be formation-rate limited. The MR of LY485912 and LSN2406799 ranged from 0.193 to 0.220 and from 0.0710 to 0.107, respectively, after multiple dosing. Systemic exposure of these metabolites was smaller than that of enzastaurin.

The intra-patient (within-subject) variability assessed using AUC for enzastaurin and its metabolites ranged from 17% to 40%. The inter-subject variability was high and ranged from 56% to108% as assessed by AUC. Figure 3 shows the average drug concentration of enzastaurin and its active metabolites in individual patients across all dose levels. Multiple daily doses at 500 mg, the recommended dose for phase II studies, achieved the target plasma concentration, 1400 nmol/L, in all Japanese patients. The predicted average drug concentration of enzastaurin and its active metabolites at steady-state ranged from 1680 to 5040 nmol/L.

Antitumor effect. All 23 patients were assessed for tumor response. No formal objective response occurred in accordance with RECIST. Three patients (two at 375 mg and one at 500 mg) had been treated without progressive disease for at least six cycles. Of these, one patient with gastro-intestinal stromal tumor continued therapy at 375 mg for 21 cycles. Another patient with mesothelioma showed radiographical improvement in positron emission tomography imaging using the glucose analog 2-deoxy-2-[18F]fluoro-D-glucose (18FDG) at 7 weeks after baseline (Fig. 4).

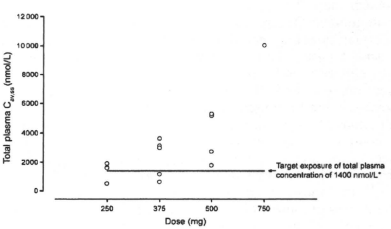

Fig. 3. Steady-state average plasma concentrations of enzastaurin and its active metabolites. *The target exposure of total plasma concentration of 1400 nmol/L was determined based on the IC90 (70 nmol/L) for protein kinase C-β inhibition by enzastaurin, assuming approximately 95% protein binding.

Discussion

In this study, we showed that enzastaurin up to 500 mg was well tolerated in Japanese patients with advanced solid tumors. Five hundred mg of enzastaurin achieved the target exposure, 1400 nmol/L, as measured by the total plasma concentration of

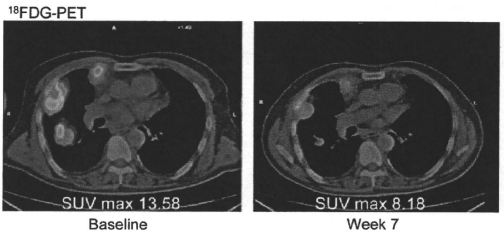

Fig. 4. Metabolic response in mesothelioma. PET, positron emission tomography; SUV, standardized uptake value.

enzastaurin and its active metabolites. In xenograft models the growth of glioblastoma and colon carcinoma were significantly suppressed by oral dosing with enzastaurin to yield plasma concentrations similar to those achieved in clinical trials.[1] On the basis of safety data and plasma exposures, we recommend a daily dose of 500 mg of enzastaurin for phase II studies in Japan. This result is consistent with results from the phase I study in non-Japanese patients.[11]

In the current study, no clinically significant toxicities other than QTc prolongation were reported. QTc prolongation was the DLT, and drug-related reversible grade 2 QTc prolongations were observed in four patients (one patient at 375 mg, one patient at 500 mg and two patients at 750 mg). The onset of each event was in cycle 0 or 1, but not on the first day of either cycle. None of these events were exacerbated during the course of treatment. Although the definitive cause of QTc prolongation is undefined, the study results are consistent with the results of a preclinical study in dogs and of the preceded phase I study in the USA. In a preclinical study in which dogs were given high daily doses (exposures higher than those expected to occur in most patients), QT and QTc prolongation was observed after 5 weeks, and cataracts were seen after 13 weeks (data on file). In the phase I study in the USA, QTc prolongation was the DLT. Events were observed at the 700 and 525 mg dose levels although they did not require treatment or discontinuation.[11] Asymptomatic QTc prolongations are reported in several novel molecular targeting oncology agents including multi-targeted tyrosine kinase inhibitors, histone deacetylase inhibitors and PKC inhibitors, and their mechanisms are being explored.[14] In recent phase II and III studies, an initial high-loading dose of enzastaurin has been used to attain steady-state plasma total concentrations of enzastaurin sooner. In such studies, it is necessary to monitor the QTc interval carefully. We are evaluating the safety of the high initial loading dose for Japanese patients in a separate study. In this study, as in another study of enzastaurin,[11] the most common toxicity observed in the treated patients was chromaturia. This is most likely due to the reddish-orange color of the active ingredient of enzastaurin.

The plasma exposures of enzastaurin in this study as assessed by AUC indicate high inter-patient variability for enzastaurin and its metabolites (56–108%) compared with intra-patient variability (17–40%). Since dose escalation was not performed within the same patients and the number of patients in each dose level was small with high variability, dose proportionality for enzastaurin and its metabolites could not be concluded.

Because this was a phase I study, efficacy was not a primary endpoint. Although formal tumor responses were not identified, one mesothelioma patient showed radiographical improvement and three patients were treated for at least six cycles without progressive disease. Phase II studies designed to measure tumor response and/or stable disease over a specified period will provide more information on the expected antitumor activity of enzastaurin.

A recent report showed that treatment with enzastaurin was well tolerated and associated with prolonged freedom from progression in a small subset of patients with relapsed or refractory DLBCL,[15] and a large global phase III trial of standard induction therapy (CHOP/rituximab) with or without enzastaurin consolidation has been initiated in patients with newly diagnosed, high-intermediate/high-risk DLBCL. Based on the results of the current study, medical institutes in Japan have joined this phase III study and investigators have been carefully monitoring all clinical aspects, including ECG.

In summary, the current study showed that enzastaurin was well tolerated up to 500 mg in Japanese patients with advanced solid tumors. The only DLT observed was reversible QTc prolongation. The recommended dose for phase II was determined to be 500 mg daily for a 28-day cycle, the same as that determined in Caucasian patients.

Acknowledgments

The authors acknowledge staff at the investigator site, Luna Musib for pharmacokinetics, and Megumi Sugiura for editorial and technical assistance.

Disclosure Statement

Financial support for this work was provided by Eli Lilly Japan, KK. Minori Koshiji and Kenichi Yoshizawa are employees of Eli Lilly Japan. None of the other authors have a conflict of interest to disclose.

Abbreviations

$AUC_{0-\infty}$	area under the concentration *vs* time curve from 0 to infinity
$AUC_{\tau,ss}$	area under the concentration *vs* time curve over the dosing interval at steady state
$C_{av,ss}$	the predicted average drug concentration under steady-state conditions during multiple dosing
CL/F	apparent total body clearance calculated after oral dosing
C_{max}	maximum plasma concentration
$C_{max,ss}$	maximum plasma concentration at steady-state
CTCAE	common terminology criteria for adverse events
ECG	electrocardiogram
ECOG	Eastern Cooperative Oncology Group
G	grade of CTCAE v3.0
GIST	gastro-intestinal stromal tumor
MedDRA	the Medical Dictionary for Regulatory Activities
MR	metabolic ratio
RA	accumulation ratio
$t_{1/2}$	half-life associated with the terminal rate constant
t_{max}	median time to reach maximum concentration
V_z/F	apparent volume of distribution after oral administration

doi: 10.1111/j.1349-7006.2010.01677.x

References

1 Graff JR, McNulty AM, Hanna KR *et al.* The protein kinase Cß-selective inhibitor, Enzastaurin (LY317615.HCl), suppresses signaling through the AKT pathway, induces apoptosis, and suppresses growth of human colon cancer and glioblastoma xenografts. *Cancer Res* 2005; **65**: 7462–9.

2 Clark AS, West KA, Blumberg PM, Dennis PA. Altered protein kinase C (PKC) isoforms in non-small cell lung cancer cells: PKCdelta promotes cellular survival and chemotherapeutic resistence. *Cancer Res* 2003; **63**: 780–6.

3 Shipp MA, Ross KN, Tamayo P *et al.* Diffuse large B-cell lymphoma outcome prediction by gene-expression profiling and supervised machine learning. *Nat Med* 2002; **8**: 68–74.

4 McMahon G. VEGF receptor signaling in tumor angiogenesis. *Oncologist* 2000; **5**(Suppl 1): 3–10.

5 Balendran A, Hare GR, Kieloch A, Williams MR, Alessi DR. Further evidence that 3-phosphoinositide-dependent protein kinase-1 (PDK1) is required for the stability and phosphorylation of protein kinase C (PKC) isoforms. *FEBS Lett* 2000; **484**: 217–23.

6 Partovian C, Simons M. Regulation of protein kinase B/Akt activity and Ser473 phosphorylation by protein kinase Calpha in endothelial cells. *Cell Signal* 2004; **16**: 951–7.

7 Wu E, Aguiar R, Savage K *et al.* PKCbeta: a rational therapeutic target in diffuse large B-cell lymphoma. *Blood* 2002; **100**: 202a.

8 Rossi RM, Henn AD, Conkling R *et al.* The PKCbeta selective inhibitor, enzastaurin (LY317615), inhibits growth of human lymphoma cells. *Blood* 2005; **106**: 427a.

9 Liu Y, Su W, Thompson EA, Leitges M, Murray NR, Fields AP. Protein kinase CbetaII regulates its own expression in rat intestinal epithelial cells and the colonic epithelium in vivo. *J Biol Chem* 2004; **279**: 45556–63.

10 Keyes K, Cox K, Treadway P *et al.* An in vitro tumor model: analysis of angiogenic factor expression after chemotherapy. *Cancer Res* 2002; **62**: 5597–602.

11 Carducci MA, Musib L, Kies MS *et al.* Phase I dose escalation and pharmacokinetic study of enzastaurin, an oral protein kinase C beta inhibitor, in patients with advanced cancer. *J Clin Oncol* 2006; **24**: 4092–9.

12 Welch PA, Sinha VP, Cleverly AL, Darstein C, Flanagan SD, Musib LC. Safety, tolerability, QTc evaluation, and pharmacokinetics of single and multiple doses of enzastaurin HCl (LY317615), a protein kinase C-beta inhibitor, in healthy subjects. *J Clin Pharmacol* 2007; **47**: 1138–51.

13 Therasse P, Arbuck SG, Eisenhauer EA *et al.* New guidelines to evaluate the response to treatment in solid tumors: European Organization for Research and Treatment of Cancer, National Cancer Institute of the United States, National Cancer Institute of Canada. *J Natl Cancer Inst* 2000; **92**: 205–16.

14 Strevel EL, Ing DJ, Siu LL. Molecularly targeted oncology therapeutics and prolongation of the QT interval. *J Clin Oncol* 2007; **25**: 3362–33671.

15 Robertson MJ, Kahl BS, Vose JM *et al.* Phase II study of enzastaurin, a protein kinase C beta inhibitor, in patients with relapsed or refractory diffuse large B-cell lymphoma. *J Clin Oncol* 2007; **25**: 1741–6.

Cancer Science
The official journal of the Japanese Cancer Association

Effect of axitinib (AG-013736) on fatigue, thyroid-stimulating hormone, and biomarkers: A phase I study in Japanese patients

Toru Mukohara,[1,4] Hikaru Nakajima,[1] Hirofumi Mukai,[1] Shunji Nagai,[1] Kuniaki Itoh,[1] Yoshiko Umeyama,[2] Junichi Hashimoto[2] and Hironobu Minami[1,3,4,5]

[1]National Cancer Center Hospital East, Oncology/Hematology, Kashiwa; [2]Pfizer Japan Inc., Tokyo, Japan

(Received November 6, 2009/Accepted December 2, 2009/Online publication February 22, 2010)

Axitinib is an oral, potent, and selective inhibitor of vascular endothelial growth factor receptor (VEGFR) 1, 2, and 3. This phase I study evaluated the safety, pharmacokinetics, pharmacodynamics, antitumor activity, and recommended starting dose of axitinib in patients with advanced solid tumors. Twelve patients received single-dose axitinib 5 mg and were monitored for ≥48 h. Continuous 5 mg twice-daily dosing was then initiated. One patient had dose-limiting toxicity (grade 3 proteinuria and fatigue). Common treatment-related adverse events were anorexia, fatigue, and diarrhea. Grade 3 treatment-related adverse events were fatigue and hypertension. Maximum axitinib plasma concentration occurred 1–4 h after steady-state dosing. Eleven patients experienced thyroid-stimulating hormone elevation; time-course change and fatigue onset appeared to be related in some patients. Significant correlation was observed between thyroid-stimulating hormone change and area under the plasma concentration–time curve (AUC; $r = 0.80$, $P = 0.005$). Axitinib decreased plasma soluble vascular endothelial growth factor receptor 2 (s-VEGFR2), with significant correlation between change in s-VEGFR2 and AUC ($r = -0.92$, $P < 0.0001$). Fluorodeoxyglucose positron emission tomography revealed a substantial decrease in tumor metabolic activity associated with axitinib. Tumor size decreased in nine patients. The time-course of thyroid-stimulating hormone change appeared correlated with fatigue. There were significant correlations between thyroid-stimulating hormone or s-VEGFR2 and axitinib exposure. Axitinib 5 mg twice-daily is the recommended starting dose for Japanese patients. This trial is registered with ClinicalTrials.gov, identifier NCT00447005. (*Cancer Sci* 2010; 101: 963–968)

Cancer fatality is usually due to tumor growth accompanied by invasion of adjacent tissues and subsequent metastatic spread. Both tumor growth and metastasis are dependent on angiogenesis,[1,2] in which vascular endothelial growth factor (VEGF), and its tyrosine kinase receptors (VEGFRs), play key regulatory roles.[3,4] Many cancers are known to secrete VEGF, which binds to VEGFRs on the surface of endothelial cells, enhancing their growth and survival. This system stimulates neovascularization towards the tumor, which provides the tumor oxygen and nutrition as well as the path for metastasis. Therefore, disrupting this system is potentially an efficacious approach in cancer therapy.

Axitinib (AG-013736) is an oral, potent, and selective inhibitor of VEGFR 1, 2, and 3.[5] Axitinib can inhibit platelet-derived growth factor receptor (PDGFR) and stem-cell factor receptor (KIT) but with a log lower potency.[5] Axitinib dose-dependently blocks VEGF-stimulated receptor autophosphorylation, leading to inhibition of endothelial cell proliferation and survival.[5] In preclinical studies, axitinib had antiangiogenic and antitumor activity in numerous human tumor types[5,6] and showed antitumor effects in combination with docetaxel, carboplatin, gemcitabine, and bevacizumab.[5]

In the first-in-human phase I study,[7] there was clear evidence of clinical activity, and the maximum tolerated dose was identified as 5 mg twice daily (BID); this dose was selected for use in phase II studies.[7] Phase II studies have confirmed that axitinib has clinical activity as a single agent and in combination with chemotherapy in various tumor types,[8–13] and axitinib is currently in phase III development in patients with metastatic renal cell carcinoma (RCC).

The primary objective of this phase I study was to determine the recommended axitinib starting dose in Japanese patients with advanced solid tumors. Secondary objectives included evaluation of axitinib plasma pharmacokinetics in the Japanese patient population and investigation of the antitumor activity of axitinib. Pharmacodynamic exploration of the plasma concentrations of soluble (s)-VEGFR2, s-VEGFR3, s-KIT, and VEGF and fluorodeoxyglucose positron emission tomography (FDG-PET) scans were also included. In addition, the effect of axitinib on thyroid function was prospectively evaluated.

Materials and Methods

Patients. Patients aged 20–75 years with histologically or cytologically documented advanced solid tumors, refractory to standard therapies or for whom no standard therapies existed, were eligible for the study. Patients were required to have Eastern Cooperative Oncology Group performance status 0–2. Eligible patients also had adequate bone marrow, hepatic, and renal function, with systolic blood pressure (BP) ≤130 mmHg and diastolic BP ≤80 mmHg, regardless of the use of antihypertensive agents.

Exclusion criteria included: central lung lesions involving major blood vessels, current or likely need for treatment with a potent cytochrome P450 (CYP) 3A4 inhibitor or CYP3A4 or CYP1A2 inducer, need for regular treatment with drugs affecting platelet function, active seizure disorder or brain metastases with symptoms or requiring treatment, clinically evident gastrointestinal disorders potentially affecting ingestion or absorption, grade ≥3 hemorrhage (based on Common Terminology Criteria for Adverse Events [CTCAE], version 3.0) ≤4 weeks prior to enrolment, and hemoptysis >1/2 teaspoon per day ≤1 week prior to enrolment.

Study design. This was an open-label, non-randomized study in patients with advanced solid tumors. The study protocol was approved by the Institutional Review Board of the National

[3]To whom correspondence should be addressed.
E-mail: hminami@med.kobe-u.ac.jp
[4]Present address: Kobe University Hospital, Cancer Center.
[5]Present address: Kobe University Hospital, Medical Oncology, 7-5-2, Kusunoki-cho, Chuo-ku, Kobe, 650-0017, Japan.

doi: 10.1111/j.1349-7006.2009.01465.x

Cancer Center, Japan, and all patients gave written informed consent for participation. The study was conducted in accordance with the Declaration of Helsinki and in accordance with the International Conference on Harmonisation guideline on Good Clinical Practice, and applicable local regulatory requirements and laws.

Six patients were initially enrolled. They received a single dose of axitinib 5 mg and were monitored for ≥48 h. Once the safety of single-dose axitinib was confirmed, continuous 5 mg BID dosing was initiated for these six patients. If axitinib was well tolerated (≤1/6 patients experienced dose-limiting toxicity [DLT]), six additional patients would be enrolled at this dose. Axitinib was administered orally in a fed state.

If a patient tolerated axitinib 5 mg BID well for ≥28 days, their dose could be increased to 7 mg BID and then to a maximum of 10 mg BID. Intra-patient dose titration was permitted if no treatment-related adverse events (AEs) grade >2 were observed and BP was ≤150/90 mmHg for 2 consecutive weeks without use of antihypertensive agents. Patients continued treatment until intolerable toxicity, progressive disease, or withdrawal of consent. Axitinib dosing was reduced or interrupted if drug-related toxicity occurred according to predefined dose-modification criteria. No other chemotherapy, hormonal therapy, or radiotherapy was permitted during the study.

Study assessments. Toxicities were evaluated according to CTCAE, version 3.0. DLT was defined as a treatment-related AE of: grade 4 neutropenia >7 days; grade 4 thrombocytopenia; grade ≥3 non-hematological toxicities except those that could be controlled to grade ≤2; hemoptysis >1/2 teaspoon per day, unless it resolved to baseline within 7 days; or proteinuria ≥2 g/day. DLT was evaluated in the first 4 weeks of continuous dosing. Patients who had ≥75% treatment compliance were considered evaluable for DLT. Laboratory investigations, including thyroid-stimulating hormone (TSH) measurement for assessment of thyroid function, were performed at screening, pre- and post-single dosing, weekly during the first 4 weeks of continuous dosing (and subsequently every 2 weeks), and at the end of study treatment. A 12-lead electrocardiogram was performed at screening, on day 15 (1–3 h post-dose), and at the end of study treatment.

Blood samples for pharmacokinetic assessment were obtained during single dosing (pre-dose, and 0.5, 1, 2, 4, 6, 8, 12, 24, and 32 h post-dose) and on days 1 and 15 of continuous dosing (pre-dose, and 0.5, 1, 2, 4, 8, and 12 h post-dose); pre-dose sampling was also performed on day 29 to evaluate trough concentration. Plasma axitinib concentrations were measured using a validated liquid chromatography-tandem mass spectrometric method (lower limit of quantification, 0.1 ng/mL) at Charles River Laboratories (Worcester, MA, USA). Standard plasma pharmacokinetic parameters were estimated using noncompartmental methods (WinNonlin Professional version 4.1, Pharsight, Mountain View, CA, USA). Pharmacokinetic parameters assessed following single and continuous dosing included maximum plasma concentration (C_{max}); area under the plasma concentration–time curve from time zero to infinity (AUC_{inf}); time to first occurrence of C_{max} (T_{max}); and terminal-phase plasma half-life ($t_{1/2}$). AUC over dosing interval $_{\tau}$(AUC12; AUC from zero to 12 h), and accumulation ratio (R_{ac}) were also evaluated following continuous dosing.

For pharmacodynamic assessments, plasma biomarkers (s-VEGFR2, s-VEGFR3, s-KIT, and VEGF) were measured pre-dose, every 4 weeks, and at the end of study treatment. Soluble proteins were analyzed by enzyme-linked immunosorbent assay at Alta Analysis (San Diego, CA, USA). Pharmacodynamic evaluation using FDG-PET was performed pre-dosing and 1–2 months after the initiation of axitinib 5 mg BID in selected patients. FDG-PET images were obtained 60 min after injection of 18F-fluorodeoxyglucose. Percentage changes in maximal standardized uptake value (SUV_{max}, corrected for body weight) were calculated.

Tumor measurements were performed at screening, every 8 weeks during continuous dosing, and at the end of study treatment. Tumor response was assessed according to the Response Evaluation Criteria in Solid Tumors.[14]

Exploratory analyses evaluated relationships between pharmacokinetic parameters and pharmacodynamic markers, and between pharmacokinetic parameters and TSH change.

Table 1. Demographic and baseline characteristics

	n = 12
Mean (range) age, years	60 (32–75)
Mean (range) weight, kg	60 (44–83)
Mean (range) height, cm	163 (149–180)
Mean (range) BSA, m^2	1.6 (1.4–2.0)
Gender, *n* (%)	
Male	7 (58)
Female	5 (42)
ECOG PS, *n* (%)	
0	6 (50)
1	5 (42)
2	1 (8)
Tumor type, *n* (%)	
Colorectal cancer	6 (50)
RCC	2 (17)
Other†	4 (33)
Prior treatment with antihypertensive agent, *n* (%)	
Yes	6 (50)
No	6 (50)

†Ovarian cancer; liposarcoma; non-small-cell lung cancer; thymic cancer. BSA, body surface area; ECOG PS, Eastern Cooperative Oncology Group performance status; RCC, renal cell carcinoma.

Results

Patient disposition and characteristics. Twelve Japanese patients with advanced solid tumors received a starting dose of axitinib 5 mg BID (Table 1). All patients had received prior systemic therapy (seven patients, 58%, had received >3 regimens), and the majority had undergone prior surgery (11 patients, 92%).

Safety. The median duration of axitinib treatment was 128 (range, 49 to 795) days. DLTs were observed in one patient, who had grade 3 proteinuria (6.4 g/day) 27 days after, and grade 3 fatigue 30 days after starting treatment with axitinib 5 mg BID. Axitinib treatment was interrupted due to proteinuria, and was resumed at a lower dose of 3 mg BID, but proteinuria (9.2 g/day) recurred 7 days later. Axitinib treatment was again interrupted, and resumed at 1 mg BID; however, proteinuria (7.8 g/day) recurred 7 days later, after which axitinib was permanently discontinued. While the other patients did not discontinue axitinib treatment due to AEs, five patients (42%) had a dose reduction due to AEs after the initial 28 days of therapy. One patient (8%) had a dose increase to 7 mg BID, and subsequently 10 mg BID. Treatment compliance during the first 28 days of treatment was 93–100%, except in one patient who experienced a DLT (79%) and in one patient with a dose interruption due to an unrelated liver abscess (66%). Seven patients (58%) were 100% compliant.

Common treatment-related AEs were anorexia, fatigue, diarrhea, stomatitis, hand–foot syndrome, hoarseness, and hypertension (Table 2). Grade 3 treatment-related AEs were fatigue and hypertension. Common treatment-related laboratory abnormalities were increased TSH and hematuria (Table 2). Grade 3 treatment-related laboratory abnormalities were increased

doi: 10.1111/j.1349-7006.2009.01465.x

Table 2. Common treatment-related adverse events and laboratory abnormalities (n = 12)

	All grades, n (%)	Grade 3†, n (%)
Adverse events		
Anorexia	11 (92)	0
Fatigue	10 (83)	5 (42)
Diarrhea	9 (75)	0
Stomatitis	8 (67)	0
Hand–foot syndrome	8 (67)	0
Hoarseness	7 (58)	0
Hypertension	6 (50)	3 (25)
Constipation	5 (42)	0
Nausea	3 (25)	0
Epistaxis	3 (25)	0
Rash	3 (25)	0
Laboratory abnormalities‡		
TSH increased	9 (75)	0
Hematuria	7 (58)	0
Proteinuria	5 (42)	1 (8)
Blood glucose increased	5 (42)	0
Lipase increased	5 (42)	0
Alkaline phosphatase increased	4 (33)	1 (8)
TSH decreased	4 (33)	0
AST increased	4 (33)	0
Free T3 increased	3 (25)	0
Free T4 increased	3 (25)	0
Hematological toxicities‡		
Thrombocytopenia	5 (42)	0
Leukopenia	3 (25)	0
Lymphopenia	1 (8)	0
Neutropenia	1 (8)	0
Anemia	0	0

†No grade 4/5 events were reported. ‡Treatment-related adverse events judged by the investigators based on laboratory tests. AST, aspartate aminotransferase; T3, tri-iodothyronine; T4, thyroxine; TSH, thyroid-stimulating hormone.

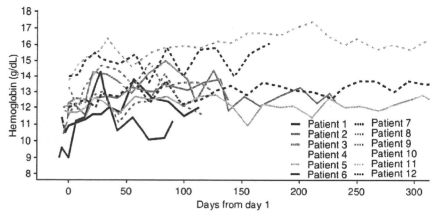

Fig. 1. Time-course of hemoglobin levels for each patient.

alkaline phosphatase, hypoalbuminemia, and proteinuria, in one patient (8%) each. All treatment-related hematological toxicities were grade 1 or 2 (Table 2). Elevation of hemoglobin was observed in most patients. The mean hemoglobin levels of 11.93 g/dL (range, 9.0 to 14.0 g/dL) at baseline increased to 13.63 g/dL (range, 11.6 to 16.4 g/dL) after 28 days of axitinib treatment and remained slightly elevated thereafter. The time-course of hemoglobin levels for each patient are presented in Figure 1.

An increase of approximately 16 mmHg (mean change from baseline) in both systolic and diastolic BP was observed (16.2 mmHg [range, 1 to 42 mmHg] in systolic BP, 16.5 mmHg [range, 3 to 32 mmHg] in diastolic BP) in patients within 1 week after the start of axitinib treatment. BP subsequently remained relatively stable. Increased BP was manageable with antihypertensive agents. No prolongation of QTc interval was observed at 1–3 h after dosing (around C_{max}) at steady state (day 15).

Pharmacokinetics. Plasma pharmacokinetic parameters for axitinib after single and continuous dosing are summarized in Table 3. C_{max} was reached 1–4 h after dosing at steady state (day 15). The mean (% coefficient of variation) R_{ac} after continuous dosing was 1.54 (32%), consistent with the value predicted from the mean half-life of axitinib.

Thyroid-stimulating hormone (TSH). Elevation of TSH above the upper limit of the normal (ULN) range was observed in most patients following axitinib treatment (11/12 patients; Fig. 2A,B). Both increased and decreased TSH were observed (Fig. 2B). Free T3/T4 was measured when clinically indicated. A decrease in free T3 and/or T4 was observed in seven patients. The time-course of TSH change and fatigue onset appeared correlated in some patients: highly elevated TSH (112 μIU/mL) occurred in one patient who experienced a DLT of grade 3 fatigue, and four patients experienced grade 3 fatigue at, or shortly after, a peak in TSH levels (Fig. 2C). A statistically significant correlation was observed between TSH change from baseline to day 29 (absolute log ratio) and day 15 AUC12 (r = 0.80; 95% confidence interval [CI]: 0.353 to 0.952; P = 0.005; excludes two patients with abnormal TSH at baseline; Fig. 2D). The absolute log ratio was used for the analyses of TSH change, as TSH values appeared to have a log-normal distribution; after logarithmic transformation, TSH followed a bell-shaped, symmetrical distribution.

Pharmacodynamics. Axitinib increased VEGF and decreased plasma s-VEGFR2 and s-VEGFR3. The median (range) change in plasma concentration from baseline to day 29 was +267% (15% to 1031%) for VEGF, −42% (−53% to −10%) for s-VEGFR2, and −53% (−94% to −16%) for s-VEGFR3. No s-KIT change was observed (median [range] change from baseline to day 29, −0.4% [−24% to 33%]). There was no correlation between change in VEGF from baseline to day 29 and AUC12; however, a decrease in s-VEGFR3 over this period was correlated with AUC12 (r = −0.82; 95% CI: −0.982 to −0.655; P = 0.001), and a significant correlation was observed between decrease in s-VEGFR2 over this period and AUC12 (r = −0.92; 95% CI: −1.000 to −0.806, P < 0.0001; Fig. 3).

FDG-PET was performed in nine patients; SUV_{max} decreased in eight patients, with a median percentage change from baseline of −52% (range, −69% to 126%). FDG-PET imaging from a patient with colorectal cancer (CRC), whose FDG uptake was significantly decreased after the treatment, is presented in Figure 4.

Antitumor activity. Although none of the 12 patients achieved a confirmed partial response, target lesion size decreased from baseline in 9/12 patients (5/6 with CRC, 1/2 with RCC, 1/1 with ovarian cancer, 1/1 with non-small-cell lung cancer (NSCLC), and 1/1 with thymic cancer), with a maximum percentage decrease of 36% (in a patient with CRC). One patient with RCC experienced a transient increase in tumor size of 70% while receiving axitinib 7 mg BID and, following dose titration to 10 mg BID, the tumor decreased by 14% compared with maximum tumor size before the dose titration to 10 mg BID. Stable disease (SD) ≥24 weeks was observed in three patients (with CRC, NSCLC, and thymic cancer [n = 1 each]); two of these patients had SD ≥52 weeks (those with NSCLC and thymic cancer).

Discussion

In this phase I study, the recommended starting dose in Japanese patients was confirmed to be identical to that used in global

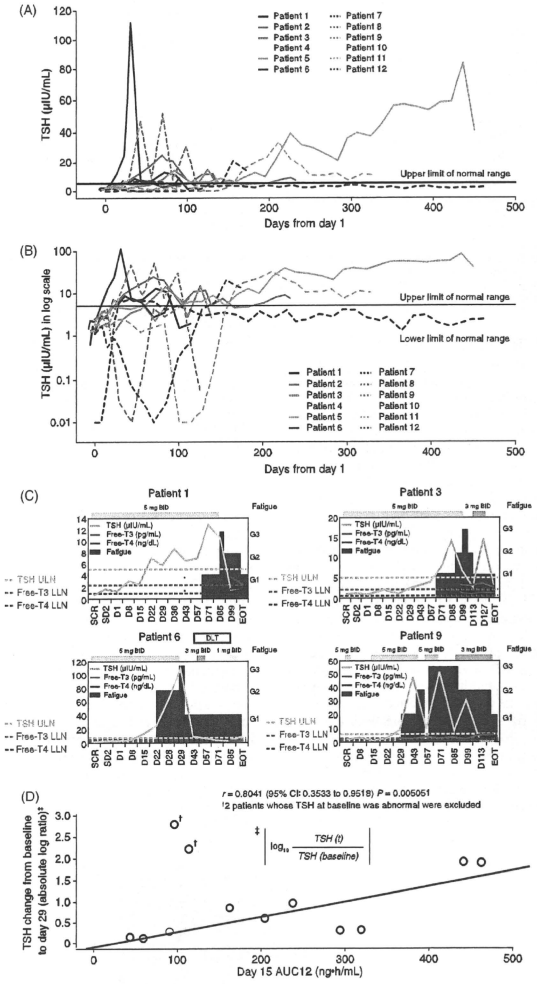

Fig. 2. Analysis of change in thyroid-stimulating hormone (TSH). TSH levels over time by patient (A, absolute values; B, log scale); (C) Relationship between TSH change and onset time of fatigue; (D) TSH change from baseline to day 29 (absolute log ratio) and area under the plasma concentration–time curve from zero to 12 h (AUC12) (n = 12). BID, twice daily; CI, confidence interval; D, day; DLT, dose-limiting toxicity; EOT, end of treatment; G, grade; LLN, lower limit of normal; SCR, screening; SD2, single dose day 2; T3, tri-iodothyronine; T4, thyroxine; ULN, upper limit of normal.

phase II and III studies (5 mg BID). This dose was well tolerated overall, with only one patient experiencing DLTs (grade 3 proteinuria and fatigue); this patient had highly elevated TSH (112 μIU/mL) and grade 3 fatigue (defined as a DLT) that may have been associated with TSH elevation. Common treatment-related AEs and laboratory abnormalities were anorexia, fatigue,

doi: 10.1111/j.1349-7006.2009.01465.x

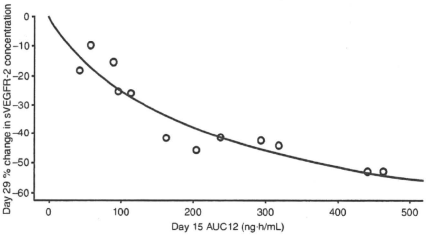

Fig. 3. Relationship between percentage change in soluble vascular endothelial growth factor receptor 2 (s-VEGFR2) level from baseline to day 29 and area under the plasma concentration–time curve from zero to 12 h (AUC12) (n = 12).

Table 3. Summary of pharmacokinetic parameters

Single dose (5 mg, fed state, up to 32 h of monitoring), n = 6				
	C_{max} (ng/mL)	AUC_{inf} (ng·h/mL)	T_{max} (h)‡	$t_{1/2}$ (h)
Mean†	28.6	181	4	4.80
CV (%)	33	70	(2, 6)	24
Day 1 (5 mg BID, fed state), n = 12				
	C_{max} (ng/mL)	AUC12 (ng·h/mL)		T_{max} (h)‡
Mean†	20.7	111		3
CV (%)	46	61		(2, 4)
Day 15 (5 mg BID, fed state), n = 11§				
	C_{max} (ng/mL)	AUC12 (ng·h/mL)	T_{max} (h)‡	R_{ac}
Mean†	27.0	150	4	1.54
CV (%)	56	67	(1, 4)	32

†C_{max}, AUC_{inf}, AUC12: geometric mean; $t_{1/2}$: arithmetic mean.
‡Median (min, max). §One patient was excluded from descriptive analysis because of lack of compliance. AUC_{inf}, AUC (area under the plasma concentration–time curve) from time zero to infinity; AUC12, AUC from zero to 12 h; BID, twice daily; C_{max}, maximum plasma concentration; CV, coefficient of variation; R_{ac}, accumulation ratio; $t_{1/2}$, terminal-phase plasma half-life; T_{max}, time to first occurrence of C_{max}.

diarrhea, and increased TSH. The only grade 3 treatment-related AEs or laboratory abnormalities were fatigue, hypertension, increased alkaline phosphatase, hypoalbuminemia, and proteinuria. All hematological toxicities were grade 1 or 2. Mean levels of hemoglobin increased from baseline by 14.2% after 28 days of initiation of axitinib treatment and remained elevated at a stable level throughout the study. No patients required treatment for elevation of hemoglobin and continued axitinib treatment did not further increase hemoglobin levels. The observed elevations of hemoglobin are consistent with hemoglobin data reported for a single patient treated with axitinib[15] and for patients treated with the multi-targeted VEGFR inhibitors sunitinib and sorafenib.[16,17] The mechanism underlying the elevation of hemoglobin associated with treatment of patients with multi-targeted VEGFR inhibitors is currently unknown. However, it has been speculated that blockade of VEGF signaling may modulate erythropoietin expression,[15,17] or VEGFR2 inhibition and subsequent reduction of nitric oxide may result in loss of intravascular fluid.[16] The pattern of BP change observed in the current study, an increase in BP within 1 week of the start of axitinib, followed by relative stability, was similar to that seen in a previous phase I study of axitinib in Caucasian patients.[7] Importantly, increases in BP were manageable with antihypertensive medication.

Maximum axitinib plasma concentrations were achieved rapidly (1–4 h) after steady-state dosing with 5 mg BID and steady-state plasma concentrations were predictable from day 1. There was minimal evidence of axitinib accumulation following continuous dosing. The steady-state pharmacokinetics of axitinib (C_{max}, AUC12) were similar to those observed in a previous phase I study in Caucasian patients.[7] Several other VEGFR tyrosine kinase inhibitors are approved or currently in clinical development, including sunitinib, sorafenib, recentin (AZD2171),[18] motesanib diphosphate (AMG706), and vandetanib. Half-lives vary considerably between these agents, ranging from 2–5 h for axitinib[7] up to 120 h for vandetanib.[19] The short half-life of axitinib allows for rapid management of AEs through treatment interruption or discontinuation.

Evidence of TSH elevation in patients with cancer has been reported in studies of other VEGFR inhibitors, including sunitinib, sorafenib, and AZD2171.[20–23] The current study is the first to evaluate TSH change following axitinib treatment. Elevation of TSH was generally observed within 1 month of axitinib treatment, and rapidly normalized or returned almost to the ULN, following dose interruption. The time-course of TSH change and fatigue onset appeared correlated in some patients, suggesting that fatigue may be related to hypothyroidism in these cases. A decrease in TSH was observed in five patients; in three

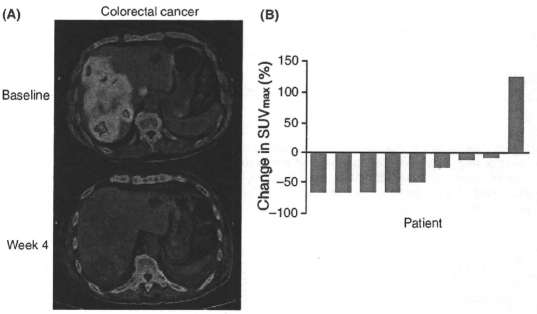

Fig. 4. Fluorodeoxyglucose positron emission tomography. (A) Imaging from the patient with colorectal cancer; (B) Percentage change in maximal standardized uptake value (SUV_{max}) by patients.

patients decreased TSH persisted for 5–8 weeks, normalized, and then increased above the ULN following further continuous treatment with axitinib. The remaining two patients discontinued treatment due to disease progression after decreased TSH was observed, and further TSH changes following continuous treatment could not be monitored. This finding suggests that the decrease in TSH was transient and may have preceded hypothyroidism with extended treatment in most patients. Desai *et al.* also reported that some patients with gastrointestinal stromal tumors receiving sunitinib experienced low TSH concentrations before developing hypothyroidism, suggesting possible thyroiditis-induced thyrotoxicosis through follicular cell apoptosis.[20] Destructive thyroiditis (also known as subacute thyroiditis) is a self-limiting form of thyrotoxicoxis due to release of preformed thyroid hormone by destruction of thyroid follicular cells.[24] Faris *et al.* suggested that treatment with sunitinib may lead to destructive thyroiditis, ultimately causing hypothyroidism.[25] Inhibition of VEGFR reduced vascular density in normal mouse thyroid.[26] It is postulated that VEGFR inhibitors, including axitinib, may induce subacute thyroiditis and hypothyroidism due to a direct effect on the thyroid through the inhibition of VEGFR. Another ongoing axitinib phase I Japanese study includes measurement of thyroglobulin levels in order to evaluate this hypothesis further. In the present study, a significant correlation was observed between change in TSH from baseline to day 29 and AUC12 ($r = 0.80$, $P = 0.005$).

Axitinib increased VEGF, and decreased s-VEGFR2 and s-VEGFR3 after 1 month of treatment; these results were consistent with those reported in patients with advanced thyroid cancer.[10] A significant correlation was observed between decrease in s-VEGFR2 from baseline and AUC12 ($r = -0.92$; $P < 0.0001$), suggesting that s-VEGFR2 levels may potentially also act as a biomarker of axitinib exposure. Additionally, in the majority of patients in whom FDG-PET was performed, SUV_{max} was decreased, with a median percentage change from baseline of −52%, indicating a substantial decrease in tumor metabolic activity associated with axitinib therapy. Confirming the antitumor activity of axitinib, a decrease in tumor size was also observed in the majority of patients following treatment.

In conclusion, fatigue and abnormal TSH levels were frequently observed and the time-course of TSH change appeared correlated with fatigue in some patients. There were significant correlations between TSH change or decrease in s-VEGFR2 level and axitinib exposure. Antitumor activity was observed in the majority of patients. Axitinib 5 mg BID, the recommended starting dose in Caucasian patients, was well tolerated and is also the recommended starting dose for Japanese patients.

Acknowledgments

This work was supported by funding from Pfizer Japan Inc., Tokyo, Japan. The authors thank medical writers at ACUMED (Tytherington, UK) for assistance in drafting the manuscript, funded by Pfizer Inc.

Disclosure Statement

This work was supported by funding from Pfizer Japan Inc., Tokyo, Japan. Toru Mukohara, Hikaru Nakajima, Hirofumi Mukai, Shunji Nagai, Kuniaki Itoh, and Hironobu Minami have nothing to disclose. Yoshiko Umeyama and Junichi Hashimoto are employees of Pfizer.

References

1 Folkman J. What is the evidence that tumors are angiogenesis dependent? *J Natl Cancer Inst* 1990; **82**: 4–6.
2 Folkman J. The role of angiogenesis in tumor growth. *Semin Cancer Biol* 1992; **3**: 65–71.
3 Hicklin DJ, Ellis LM. Role of the vascular endothelial growth factor pathway in tumor growth and angiogenesis. *J Clin Oncol* 2005; **23**: 1011–27.
4 Ferrara N, Gerber HP, LeCouter J. The biology of VEGF and its receptors. *Nat Med* 2003; **9**: 669–76.
5 Hu-Lowe DD, Zou HY, Grazzini ML *et al.* Nonclinical anti-angiogenesis and anti-tumor activity of axitinib, an oral, potent, and selective inhibitor of VEGF receptor tyrosine kinases 1, 2, 3. *Clin Cancer Res* 2008; **14**: 7272–83.
6 Wilmes LJ, Pallavicini MG, Fleming LM *et al.* AG-013736, a novel inhibitor of VEGF receptor tyrosine kinases, inhibits breast cancer growth and decreases vascular permeability as detected by dynamic contrast-enhanced magnetic resonance imaging. *Magn Reson Imaging* 2007; **25**: 319–27.
7 Rugo HS, Herbst RS, Liu G *et al.* Phase I trial of the oral antiangiogenesis agent AG-013736 in patients with advanced solid tumors: pharmacokinetic and clinical results. *J Clin Oncol* 2005; **23**: 5474–83.
8 Rini BI, Wilding G, Hudes G *et al.* Phase II study of axitinib in sorafenib-refractory metastatic renal cell carcinoma. *J Clin Oncol* 2009; **27**: 4462–8.
9 Rixe O, Bukowski RM, Michaelson MD *et al.* Axitinib treatment in patients with cytokine-refractory metastatic renal-cell cancer: a phase II study. *Lancet Oncol* 2007; **8**: 975–84.
10 Cohen EE, Rosen LS, Vokes EE *et al.* Axitinib is an active treatment for all histologic subtypes of advanced thyroid cancer: results from a phase II study. *J Clin Oncol* 2008; **26**: 4708–13.
11 Schiller JH, Larson T, Ou SH *et al.* Efficacy and safety of axitinib in patients with advanced non-small-cell lung cancer: results from a phase II study. *J Clin Oncol* 2009; **27**: 3836–41.
12 Fruehauf JP, Lutzky J, McDermott DF *et al.* Axitinib (AG-013736) in patients with metastatic melanoma: a phase II study (abstract). *J Clin Oncol* 2008; **26**: 484s.
13 Rugo HS, Stopeck A, Joy AA *et al.* A randomized, double-blind phase II study of the oral tyrosine kinase inhibitor (TKI) axitinib (AG-013736) in combination with docetaxel (DOC) compared to DOC plus placebo (PL) in metastatic breast cancer (MBC) (abstract). *J Clin Oncol* 2007; **25**: 32s.
14 Therasse P, Arbuck SG, Eisenhauer EA *et al.* New guidelines to evaluate the response to treatment in solid tumors. European Organization for Research and Treatment of Cancer, National Cancer Institute of the United States, National Cancer Institute of Canada. *J Natl Cancer Inst* 2000; **92**: 205–16.
15 Alexandre I, Billemont B, Meric JB, Richard S, Rixe O. Axitinib induces paradoxical erythropoietin synthesis in metastatic renal cell carcinoma. *J Clin Oncol* 2009; **27**: 472–3.
16 van der Veldt AA, Boven E, Vroling L, Broxterman HJ, van den Eertwegh AJ, Haanen JG. Sunitinib-induced hemoglobin changes are related to the dosing schedule. *J Clin Oncol* 2009; **27**: 1339–40.
17 Alexandrescu DT, McClure R, Farzanmehr H, Dasanu CA. Secondary erythrocytosis produced by the tyrosine kinase inhibitors sunitinib and sorafenib. *J Clin Oncol* 2008; **26**: 4047–8.
18 Laurie SA, Gauthier I, Arnold A *et al.* Phase I and pharmacokinetic study of daily oral AZD2171, an inhibitor of vascular endothelial growth factor tyrosine kinases, in combination with carboplatin and paclitaxel in patients with advanced non-small-cell lung cancer: the National Cancer Institute of Canada clinical trials group. *J Clin Oncol* 2008; **26**: 1871–8.
19 Holden SN, Eckhardt SG, Basser R *et al.* Clinical evaluation of ZD6474, an orally active inhibitor of VEGF and EGF receptor signaling, in patients with solid, malignant tumors. *Ann Oncol* 2005; **16**: 1391–7.
20 Desai J, Yassa L, Marqusee E *et al.* Hypothyroidism after sunitinib treatment for patients with gastrointestinal stromal tumors. *Ann Intern Med* 2006; **145**: 660–4.
21 Tamaskar I, Bukowski R, Elson P *et al.* Thyroid function test abnormalities in patients with metastatic renal cell carcinoma treated with sorafenib. *Ann Oncol* 2008; **19**: 265–8.
22 Rini BI, Tamaskar I, Shaheen P *et al.* Hypothyroidism in patients with metastatic renal cell carcinoma treated with sunitinib. *J Natl Cancer Inst* 2007; **99**: 81–3.
23 Drevs J, Siegert P, Medinger M *et al.* Phase I clinical study of AZD2171, an oral vascular endothelial growth factor signaling inhibitor, in patients with advanced solid tumors. *J Clin Oncol* 2007; **25**: 3045–54.
24 Lazarus JH. Silent thyroiditis and subacute thyroiditis. In: Braverman L, Utiger RD, eds. *Werner and Ingbar's The Thyroid – A Fundamental and Clinical Text*, 7th edn. Philadelphia, PA: Lippincott-Raven Publishing, 1996; 577–91.
25 Faris JE, Moore AF, Daniels GH. Sunitinib (sutent)-induced thyrotoxicosis due to destructive thyroiditis: a case report. *Thyroid* 2007; **17**: 1147–9.
26 Kamba T, Tam BY, Hashizume H *et al.* VEGF-dependent plasticity of fenestrated capillaries in the normal adult microvasculature. *Am J Physiol Heart Circ Physiol* 2006; **290**: H560–76.

doi: 10.1111/j.1349-7006.2009.01465.x

original article

Annals of Oncology 21: 255–262, 2010
doi:10.1093/annonc/mdp304
Published online 24 July 2009

Association between gain-of-function mutations in *PIK3CA* and resistance to HER2-targeted agents in *HER2*-amplified breast cancer cell lines

Y. Kataoka[1], T. Mukohara[2,3]*, H. Shimada[4], N. Saijo[4], M. Hirai[1] & H. Minami[2,3]

[1]*Hospital Pharmacy;* [2]*Cancer Center, Kobe University Hospital;* [3]*Medical Oncology, Department of Medicine, Kobe University Graduate School of Medicine, Chuo-ku, Kobe and* [4]*Research Center for Innovative Oncology, National Cancer Hospital East, Kashiwa, Japan*

Received 24 April 2009; accepted 4 May 2009

Background: The mechanism of resistance to human epidermal growth factor receptor 2 (HER2)-targeted agents has not been fully understood. We investigated the influence of *PIK3CA* mutations on sensitivity to HER2-targeted agents in naturally derived breast cancer cells.

Materials and methods: We examined the effects of Calbiochem (CL)-387,785, HER2 tyrosine kinase inhibitor, and trastuzumab on cell growth and *HER2* signaling in eight breast cancer cell lines showing *HER2* amplification and trastuzumab-conditioned BT474 (BT474-TR).

Results: Four cell lines with *PIK3CA* mutations (E545K and H1047R) were more resistant to trastuzumab than the remaining four without mutations (mean percentage of control with 10 μg/ml trastuzumab: 58% versus 92%; $P = 0.010$). While *PIK3CA*-mutant cells were more resistant to CL-387,785 than *PIK3CA*-wild-type cells (mean percentage of control with 1 μM CL-387,785: 21% versus 77%; $P = 0.001$), CL-387,785 retained activity against BT474-TR. Growth inhibition by trastuzumab and CL-387,785 was more closely correlated with changes in phosphorylation of S6K (correlation coefficient, 0.811) than those of HER2, Akt, or ERK1/2. Growth of most *HER2*-amplified cells was inhibited by LY294002, regardless of *PIK3CA* genotype.

Conclusions: *PIK3CA* mutations are associated with resistance to HER2-targeted agents. PI3K inhibitors are potentially effective in overcoming trastuzumab resistance caused by *PIK3CA* mutations. S6K phosphorylation is a possibly useful pharmacodynamic marker in HER2-targeted therapy.

Key words: breast cancer, HER2, *PIK3CA*, trastuzumab

introduction

Breast cancer is the leading cause of cancer death among women worldwide, with ~1 million new cases reported each year [1, 2]. Approximately 20% of breast cancer tumors show overexpression of the HER2 protein, which is mainly caused by gene amplification. HER2 overexpression has been repeatedly identified as a poor prognostic factor [3, 4]. Trastuzumab is a humanized mAb targeting the extracellular domain of the HER2 protein. From the late 1990s, clinical studies have intensively evaluated the therapeutic roles of trastuzumab. For the treatment of HER2-overexpressing metastatic breast cancers, studies report that a combination of trastuzumab and conventional chemotherapy shows significantly higher efficacy than chemotherapy alone [5]. The use of trastuzumab has extended to the treatment of operable HER2-overexpressing breast cancer as an adjuvant or neoadjuvant [6–8]. Despite promising usefulness in clinics, a modest percentage of patients are reported to benefit from trastuzumab therapy, with response rates to trastuzumab as a single agent of ~20% [9]. In addition, even when trastuzumab therapy leads to temporary tumor shrinkage, clinical relapse is observed for the vast majority of metastatic patients. To develop adequate therapies capable of overcoming primary and secondary resistance to trastuzumab, a better understanding of the resistance mechanism is crucial.

To date, several mechanisms of primary resistance to trastuzumab have been proposed. A series of studies indicated that trastuzumab resistance is due to the truncated form of HER2, which lacks an extracellular domain to which trastuzumab is indicated to attach [10, 11]. Nagata et al. [12] demonstrated that loss of phosphatase and tensin homolog deleted on chromosome 10 (PTEN), a negative regulator of PI3K, correlates with poor response to trastuzumab. More recently, the roles of *PIK3CA* in trastuzumab resistance have been under particular investigation. Somatic mutations of *PIK3CA* were first identified in 2004 in various malignant tumors including breast cancer [13]. Subsequent studies have reported that the E545K and H1047R hotspot mutations, found

Correspondence to: Dr T. Mukohara, Department of Medical Oncology, Kobe University Hospital, 7-5-2, Kusunoki-cho, Chuo-ku, Kobe 650-0017, Japan. Tel: +81-78-382-5825; Fax: +81-78-382-5821; E-mail: mukohara@med.kobe-u.ac.jp

on exons 9 and 20, respectively, are the most frequent types of mutation, found in 8%–40% of breast cancer tumors [13–16]. Both hotspot mutations are gain-of-function mutations which transform normal mammary epithelial cells [17, 18]. Berns et al. [19] investigated the roles of gain-of-function mutations of the *PIK3CA* gene in trastuzumab resistance by transfecting wild-type and mutant (H1047R) forms of *PIK3CA* in SKBR-3 HER2-overexpressing breast cancer cells. Results showed that compared with green fluorescent protein (GFP) control, both wild-type and mutant *PIK3CA* transfections resulted in trastuzumab resistance. Further, analysis of *PIK3CA* genotypes in tumor samples obtained from breast cancer patients having undergone trastuzumab-based therapy showed an association between the presence of *PIK3CA* hotspot mutations and shorter time to progression after therapy [19].

Tyrosine kinase inhibitors (TKIs) have also been investigated as potential agents against trastuzumab resistance [20]. A clinical study in metastatic breast cancer patients having previously experienced tumor progression under trastuzumab-based therapies showed that compared with capecitabine alone, treatment using a combination of capecitabine with lapatinib, a dual inhibitor of epidermal growth factor receptor (EGFR) and HER2 tyrosine kinase, lead to significantly longer time to progression [21]. Eichhorn et al. [22], however, demonstrated that transfection of mutant *PIK3CA* (H1047R) in BT474 HER2-overexpressing breast cancer cells resulted in resistance to lapatinib compared with parental cells. Further, results showed that resistance was overcome using NVP-BEZ235, a PI3K and mammalian target of rapamycin dual inhibitor [22].

These findings based on gene manipulations indicate that gain-of-function mutations in the *PIK3CA* gene lead to resistance to trastuzumab, as well as HER2-TKI. To our knowledge, however, these findings have not been confirmed in naturally derived breast cancer cells. Here, trastuzumab resistance due to *PIK3CA* mutations was evaluated in eight naturally derived breast cancer cell lines harboring *HER2* gene amplification. Further, possible therapeutic means to overcome primary and secondary resistance to trastuzumab were investigated, as well as potential pharmacodynamic markers correlated with the growth-inhibitory effect of HER2-targeted drugs.

materials and methods

cell culture

MCF-7, MDA-MB-361, HCC1954, MDA-MB-453, UACC893, CAMA-1, MDA-MB-435S, MDA-MB-415, ZR75-30, HCC70, MDA-MB-468, and HCC1419 cell lines were purchased from the American Type Culture Collection (Manassas, VA). BT474, SKBR-3, BT549, T47D, ZR75-1, and MDA-MB-231 cells were kindly provided by Ian Krop of the Dana-Farber Cancer Institute. Of the 18 breast cancer cell lines, eight (ZR75-30, BT474, SKBR-3, HCC1419, MDA-MB-453, MDA-MB-361, HCC1954, and UACC 893) were reported to have *HER2* gene amplification [23], with levels of PTEN protein expression equivalent to those reported in our previous study [24]. Among the *HER2*-amplified cell lines, ZR75-30, SKBR-3, and HCC1419 were reported to contain the wild-type *PIK3CA* gene and MDA-MB-453, MDA-MB-361, HCC1954, and UACC893 hotspot *PIK3CA* mutations (Table 1) [14]. BT474 was reported to contain a relatively rare type of *PIK3CA* mutation at exon 2, K111N (Table 1) [14]. MDA-MB-435S, MDA-MB-468, and MDA-MB-231 cells were maintained in Dulbecco's Modified Eagle's Medium (Cellgro; Mediatech, Inc., Herndon, CA) with 10% fetal bovine serum (FBS) (Gemini Bio-Products, Inc., Woodland, CA), 100 U/ml penicillin, 100 U/ml streptomycin, and 2 mM glutamine. The remaining cell lines were maintained in RPMI-1640 medium (Cellgro; Mediatech, Inc.) supplemented with 10% FBS, 100 U/ml penicillin, 100 U/ml streptomycin, and 2 mM glutamine. All cells were grown at 37°C in a humidified atmosphere with 5% CO_2 and were in logarithmic growth phase at initiation of the experiments.

Table 1. Genotype of *PIK3CA* in *HER2*-amplified breast cancer cell lines

Cell line	Genotype of *PIK3CA*
BT474	K111N
ZR75-30	wt
SKBR-3	wt
HCC1419	wt
MDA-MB-361	E545K
MDA-MB-453	H1047R
HCC1954	H1047R
UACC893	H1047R

wt, wild-type.

drugs

Trastuzumab was obtained from the Kobe University Hospital pharmacy. CL-387,785, a dual inhibitor of EGFR and HER2 [25], and LY294002, a PI3K inhibitor, were purchased from Calbiochem (San Diego, CA). Stock solutions were prepared in dimethyl sulfoxide (DMSO) and stored at −20°C. Before each experiment, drugs were diluted in fresh media. The final DMSO concentration was <0.1% for all experiments.

antibodies and western blotting

Cells were washed with ice-cold phosphate-buffered saline and scraped immediately after adding lysis buffer [20 mM Tris (pH 7.5), 150 mM NaCl, 10% glycerol, 1% Nonidet P-40, and 2 mM EDTA] containing protease and phosphatase inhibitors (100 mM NaF, 1 mM phenylmethylsulfonyl fluoride, 1 mM Na_3VO_4, 2 μg/ml aprotinin, and 5 μg/ml leupeptin). Lysates were centrifuged at 14 000 relative centrifugal force for 10 min. Supernatants were collected as protein extract and then separated by electrophoresis on 7.6% polyacrylamide–sodium dodecyl sulfate gels, followed by transfer to nitrocellulose membranes (Millipore Corporate Headquarters, Billerica, MA) and detection by immunoblotting using an enhanced chemiluminescence system (New England Nuclear Life Science Products, Inc., Boston, MA). The resulting signals were digitally quantified using the ImageJ software (www.nih.gov). Phospho-HER2/ErbB2 (Thr1221/1222), phospho-p70 S6 Kinase (Thr389), phospho-Akt (Ser473)(D9E), and PathScan(R) Multiplex Western Cocktail I were purchased from Cell Signaling Technology (Beverly, MA). The phospho-1/2 (pT185/pY187) antibody was purchased from Biosource International Inc. (Camarillo, CA), the c-erbb-2 antibody from Chemicon (Billerica, MA), and β-actin antibody from Sigma-Aldrich (St Louis, MO).

cell growth assay

Growth inhibition was assessed using the 3-(4,5-dimethylthiazol-2-yl)-5-(3-carboxymethoxyphenyl)-2-(4-sulfophenyl)-2H-tetrazolium (MTS) assay (Promega, Madison, WI), a colorimetric method for determining the number of viable cells based on the bioreduction of MTS to a soluble formazan product, which is detectable by spectrophotometry at a wavelength of 490 nm. Cells were diluted in 160 μl/well of maintenance cell culture media and plated in 96-well flat-bottom plates (Corning, Inc., Corning, NY). After a 96-h growth period, the number of cells required to obtain an absorbance of 1.3–2.2, the linear range of the assay, was

determined for each cell line beforehand. The number of cells per well used in the subsequent experiments were as follows: MCF-7, 2000; MDA-MB-361, 8000; HCC1954, 2500; MDA-MB-453, 7000; UACC893, 7500; CAMA-1, 6000; MDA-MB-435S, 2000; ZR75-30, 7500; HCC70, 4000; HCC1419, 8000; BT474, 3000; SKBR-3, 2500; BT549, 2000; T47D, 2500; ZR75-1, 7500; MDA-MB-415, 5000; and MDA-MB-231, 2500. At 24 h after plating, cell culture media were replaced with 10% FBS-containing media with and without trastuzumab or CL-387,785, followed by incubation for an additional 120 h. Trastuzumab and CL-387,785 concentrations ranged from 33 ng/ml to 100 μg/ml and from 3.3 nM to 10 μM, respectively. A total of 6–12 plate wells were set for each experimental point, and all experiments were carried out at least in triplicate. Data are expressed as percentage of growth relative to that of untreated control cells.

generation of *in vitro* BT474-TR

To generate a cell line resistant to trastuzumab, BT474 cells were continuously exposed to 100 μg/ml trastuzumab. To confirm the emergence of resistant clones, MTS assays were carried out every five passages after allowing cells to grow in drug-free conditions for at least 4 days. After 11 months of drug exposure, cells showed sufficient resistance (Figure 1) and were designated as BT474-TR. For controls, BT474 parental cells were concomitantly maintained without trastuzumab, and drug sensitivity was compared with trastuzumab-conditioned cells. No significant change in the sensitivity to trastuzumab was observed in parental cells during the drug-exposure period (data not shown).

results

inhibitory effect of trastuzumab on growth in breast cancer cell lines

We first screened 17 breast cancer cell lines for *in vitro* growth inhibition using trastuzumab. We confirmed that all relatively sensitive cell lines were *HER2*-amplified (Figure 2A). Among eight *HER2*-amplified cell lines, those with hotspot mutations in *PIK3CA* appeared resistant compared with the remaining cell lines (Figure 2B and C). We categorized BT474 as a *PIK3CA*-wild-type cell line in this study, based on reports showing that the K111N mutation lack ability of transformation and its influence on downstream signaling is negligible [18, 26]. A significant difference in sensitivity at 10 μg/ml trastuzumab was observed between *PIK3CA*-wild-type and -mutant cells (Figure 2C; $P = 0.010$). Protein expression levels of p110-α, the product of *PIK3CA*, were not correlated with sensitivity to trastuzumab (Figure 2C).

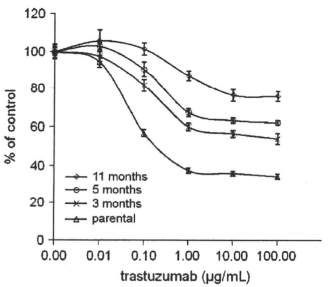

Figure 1. Development of BT474-TR. BT474 cells were continuously exposed to 100 μg/ml trastuzumab. BT-474 and trastuzumab-conditioned BT474 cells were grown in 10% serum-containing media for 5 days in the presence of various concentrations of trastuzumab. The percentage of viable cells is shown relative to that of the untreated control and plotted on the *y*-axis, whereas trastuzumab concentrations are plotted on the *x*-axis. Each data point represents the mean value and standard deviation of 6–12 replicate wells. Trastuzumab resistance increased in cells in a time-dependent manner. After 11 months, cells were designated as BT474-TR.

association between *PIK3CA* mutations and HER2-TKI resistance

Lapatinib, a HER2-TKI which may potentially overcome trastuzumab resistance, has been used in clinical settings [21]. We therefore tested a commercially available HER2-TKI, CL-387,785 [25], on *HER2*-amplified breast cancer cells. As shown in Figure 2D, cell lines with hotspot *PIK3CA* mutations showed resistance to CL-387,785. A statistically significant difference in sensitivity to 1 μM CL-387,785 was observed between *PIK3CA*-wild-type and -mutant cells (Figure 2C; $P = 0.001$) [24].

We then established a trastuzumab-resistant BT474 cell line (BT474-TR), a model of secondary resistant cells, by continuous exposure to trastuzumab (see 'Materials and methods' section). In contrast to *PIK3CA*-mutant cells, which showed primary resistance to trastuzumab, BT474-TR cells remained sensitive to CL-387,785 (Figure 3), which indicates that secondary resistant cells maintain dependency on HER2 signaling for growth.

association between phosphorylation change in S6K and growth inhibition by HER2-targeted agents

To identify potential pharmacodynamic markers of sensitivity to HER2-targeted therapy, we examined changes in phosphorylation of HER2 and representative downstream signaling molecules in 10% FBS-containing media with or without 10 μg/ml trastuzumab or 1 μM CL-387,785 (Figure 4A). The trastuzumab concentration was selected based on maintained growth inhibition (Figure 2B) and wide use in previous studies [11, 19]. The 1-μM CL-387,785 concentration was selected based on the approximate maximum plasma concentration of most TKIs available in clinics to date, including lapatinib [27], and use in previous studies [28, 29].

Trastuzumab treatment resulted in moderate phosphorylation inhibition of Akt and/or S6K in cell lines with wild-type *PIK3CA*. In contrast, no significant changes in Akt and S6K phosphorylation were observed in cell lines with hotspot mutant *PIK3CA*, as well as in BT474-TR cells. Although in ZR75-30, trastuzumab treatment appeared to inhibit phospho-ERK1/2, no significant changes were observed in other sensitive cells, namely BT474 and SKBR-3 (Figure 4A). In addition, phospho-ERK1/2 levels increased in MDA-MB-361 and UACC893, which indicates the presence of compensational cell signaling. Further, with the exception of HCC1419, treatment with CL-387,785 resulted in significant inhibition of Akt and S6K phosphorylation in BT474-TR and *PIK3CA*-wild-type cells, whereas residual phosphorylation signals were observed in all *PIK3CA* hotspot mutant cells.